1 Contributions of primary anthropogenic sources and rapid secondary

2 transformations to organic aerosol pollution in Nanchang, Central China

- Wei Guo^{a, b}, Zicong Li^{a, b}, Renguo Zhu^{a, b}, Zhongkui Zhou^a, Hongwei Xiao^c, Huayun Xiao^c
- 4 a. School of Water Resources and environmental Engineering, East China University of Technology,
- 5 Nanchang 330013, China
- 6 b. Jiangxi Province Key Laboratory of the Causes and Control of Atmospheric Pollution, East China
- 7 University of Technology, Nanchang 330013, China
- 8 c. School of Agriculture and Biology, Shanghai Jiao Tong University, Shanghai 200240, China
- 9 Correspondence: Huayun Xiao (xiaohuayun@sjtu.edu.cn)

Abstract

Owing to the complex composition of organic aerosols (OAs), elucidating their sources and dynamics is challenging, particularly in urban environments in China, where natural and anthropogenic influences converge. Herein, we attempted to clarify the relative contributions of primary emissions and secondary formations to urban OAs and confirm the sources and influencing factors of OA pollution. To achieve this, we conducted a comprehensive analysis of major polar organic compounds in samples of fine particulate matter with an aerodynamic diameter of <2.5 µm (PM_{2.5}) that were collected over a year in Nanchang, Central China. Fatty acids (FAs), fatty alcohols, and saccharides showed higher concentrations than lignin, resin products, sterols, glycerol, hydroxy acids, and aromatic acids; an analysis of molecular characteristics and concentration ratios revealed that these compounds originated from anthropogenic and natural sources. Using a tracer-based method, we observed that primary organic carbon (POC) and primary OAs (POAs) contributed 53% to the total organic-carbon content and 21% to the PM_{2.5} mass, respectively, compared with a mere 8% and 4% from secondary organic carbon (SOC) and secondary OAs (SOAs). Anthropogenic sources were the most dominant determinant, contributing approximately 89% of POC and POAs as well as 60% of SOC and SOAs. Seasonal variations indicated that biogenic emissions exerted a stronger influence during spring and summer, whereas anthropogenic emissions were more pronounced in autumn and winter. Further, short-term winter pollution

episodes were characterized by rapid secondary transformation, promoted by elevated primary emissions and favorable oxidation conditions, including increased light intensity and nitrogen oxides.

28

29

30

31

32

33

34

35

36

37

38

39

40

41

42

43

44

45

46

47

48

49

50

51

52

26

27

1 Introduction

Fine particulate matter (PM), specifically PM with an aerodynamic diameter of <2.5 µm (PM_{2.5}), affects the environment and climate, posing severe threats to human health (Huebert et al., 2003; Kanakidou, 2005; Riipinen et al., 2012; Shiraiwa et al., 2017; Yazdani et al., 2021). This is evident in China, which has become a focal point for PM_{2.5} pollution, characterized by recurrent haze episodes that have intensified since 2011 (Cao et al., 2012; Zhang et al., 2012; Huang et al., 2014). To tackle this pressing challenge, the Chinese government has implemented various measures, including the Air Pollution Prevention and Control Action Plan in 2013, revisions to the Air Pollution Prevention and Control Law in 2014, and the Three-year Action Plan for Winning the Blue Sky Defense War in 2018. Such initiatives have remarkably reduced PM2.5 levels, with concentrations below 35 µg m⁻³ as of 2020 (Figure S1a). However, the challenge persists, particularly during winter, as exemplified by the winter of 2023-2024 when PM_{2.5} concentrations in many cities exceeded the national air quality standards (Figures S1b and S1c). This underscores an urgent need for effective air quality management strategies (An et al., 2019; Cao and Cui, 2021; Chen et al., 2021; Wu et al., 2021; Zhang et al., 2024). To address urban PM_{2.5} pollution, comprehensive investigation of pollutant components, identification of pollution sources, and evaluation of influencing factors are required. Organic components constitute an important part of PM_{2.5}, accounting for 30%-50% of its mass, with primary and secondary sources (Huang et al., 2014; Zhang et al., 2016; Haque et al., 2022). Primary organic carbon (POC) or primary organic aerosol (POA) is directly emitted from various sources, including biomass burning, coal combustion, vehicle exhaust, cooking, plant debris, and fungal spores (Guo et al., 2012; Yazdani et al., 2021). Secondary organic carbon (SOC) or secondary organic aerosol (SOA) forms in the atmosphere through the photooxidation of biogenic and anthropogenic volatile organic compounds (BVOCs and AVOCs, respectively) (Lewandowski et al., 2008; Stone et al., 2009). Common biogenic precursors include hemiterpenes, monoterpenes, and sesquiterpenes, whereas typical anthropogenic precursors include toluene and polycyclic aromatic hydrocarbons (PAHs) (Claeys et al., 2004; Al-Naiema and Stone, 2017; Jaoui et al.,

2019). Owing to the complex composition of OAs, their diverse emission sources, and the impact of meteorological conditions and photochemical oxidation processes, OA source identification is complicated (Ding et al., 2013; Zhang et al., 2024). For years, research on the composition and source apportionment of OAs has attracted considerable attention. However, a unified conclusion regarding OA sources, particularly in China's intricate urban environments influenced by natural and anthropogenic factors, remains elusive (Wang et al., 2006; Fu et al., 2008; Guo et al., 2012; Ding et al., 2014; Xu et al., 2022). Various source apportionment methods have been employed. Such methods include the elemental carbon-based and water soluble OC-based methods (EC-based and WSOC-based methods, respectively; Xu et al., 2021), the compound tracer method (tracer-based method; Ding et al., 2014; Ren et al., 2021; Haque et al., 2023), the isotope signature method (Tang et al., 2022; Xu et al., 2022 and 2023; Zhang et al., 2024), and the use of source apportionment models, such as the chemical mass balance (CMB) and positive matrix factorization models (Xu et al., 2021; Zhang et al., 2023). However, these methods yielded different source contributions. The relative significance of primary emissions versus secondary formation in urban OAs continues to be controversial. Further investigation is required to clarify the sources of OA pollution and the influencing factors.

Thus, this research presents a comprehensive assessment of OAs in Nanchang, a city in Central China characterized by moderate $PM_{2.5}$ pollution levels that reflect broad urban atmospheric conditions across China (Figure S1). Employing the EC-based and tracer-based methods, as well as the CMB model, we quantitatively evaluated the contributions of POC and SOC to OC, as well as the contributions of the corresponding POA and SOA to the mass of $PM_{2.5}$. Results showed that urban OAs were predominantly influenced by anthropogenic sources, with primary contributions exceeding secondary contributions. Based on a continuous year-long observation (November 1, 2020 to October 31, 2021, 365 daily samples), we discovered that the anthropogenic contributions significantly increased in autumn and winter. However, the biogenic contributions increased in spring and summer. Short-term winter pollution episodes were promoted by rapid secondary transformation, primarily due to high primary emissions and favorable oxidation conditions, including increased light intensity and nitrogen oxides (NO_x) . This study integrates multiple source apportionment methods and accounts for the seasonal characteristics of OA pollution, providing a robust framework for understanding urban air quality dynamics. The findings have implications for governmental strategies for mitigating air pollution and

preventing haze episodes in Nanchang and its environs. The insights obtained serve as a future reference for investigating the impacts of organic compounds in $PM_{2.5}$ on visibility, public health, and climate change.

2 Materials and methods

2.1 Sampling sites and sample collection

- The study area was Nanchang, Central China, with sampling at the East China University of Technology located in the northwest region of the city (28.72°N, 115.83°E). As detailed in our previous investigations (Guo et al., 2024a and 2024b), the sampling site was in a mixed-use area characterized by educational, commercial, transportation, and residential activities, devoid of significant local pollution sources. The sampler was strategically placed on the rooftop of a six-story building, approximately 20 m in height, ensuring an unobstructed sampling environment.
- Sampling was conducted from November 1, 2020, to October 31, 2021, with daily PM_{2.5} sample collection. An 8-inch × 10-inch quartz fiber filter (Pall Tissuquartz, USA) was employed in a high-volume air sampler at a flow rate of 1.05 ± 0.03 m³ min⁻¹ for sample collection. The meteorological parameters and gaseous pollutant data for the sampling period were sourced from publicly available online monitoring platforms (https://weatherandclimate.info and http://www.aqistudy.cn/). Text S1 and Figure S2 provide a comprehensive overview of the prevalent meteorological conditions and air quality during the sampling period.

2.2 Chemical analyses

- The OC and EC concentrations in the PM_{2.5} samples were quantified using the Desert Research Institute Model 2001 Carbon Analyzer, following the thermal/optical reflectance protocol established by the Interagency Monitoring of Protected Visual Environments (IMPROVE). A 1.0-cm² filter sample was placed in a quartz boat in the analyzer and subjected to incremental heating at predetermined temperatures. Repeated analyses were performed, demonstrating an analytical uncertainty of $\pm 10\%$.
 - We employed methodologies outlined by Wang et al. (2005 and 2006) and Fu et al. (2008 and 2010) for the extraction and derivatization of organic compounds. The involved filter samples underwent three consecutive ultrasonic extractions using a dichloromethane–methanol mixture (2:1 v/v), followed by the concentration and drying of the resulting extracts. Prior to instrumental analyses, N,O-bis-(trimethylsilyl) trifluoroacetamide and pyridine were introduced to derivatize the polar compounds in the extract, with C13 n-alkanes added as

internal standards for quantitative analyses.

The identification and quantification of organic compounds were achieved via gas chromatography—mass spectrometry (GC—MS) using a Thermo Scientific TRACE GC system coupled to a Thermo Scientific ISQ QD single quadrupole mass spectrometer. GC separation was performed using a DB-5MS fused silica capillary column. Text S2 and Table S1 present the parameters for GC—MS analysis, including temperature elevation procedures, qualitative and quantitative methods for the compounds, and quality assurance and control protocols. Polar and nonpolar organic compounds in the extracts were simultaneously analyzed; however, this study focused on the results regarding the polar compounds; the findings related to nonpolar compounds are provided in our earlier publications (Guo et al., 2024a and 2024b).

2.3 Source apportionment methods

To assess the contributions of various primary and secondary sources to OC and PM_{2.5}, we employed the tracer-based method, a well-established method for source apportionment. This study focused on two types of organic tracers that serve as indicators for POC and SOC or POA and SOA. By integrating the reported ratios of specific tracers to OC and aerosol mass concentrations from various emission sources with the actual tracer concentrations measured in the present samples, we calculated the contributions of these sources to OC and PM_{2.5}. The calculation equations were as follows (Kleindienst et al., 2007 and 2012):

123
$$[POC] = \frac{\sum_{i} [tr_i]}{f_{POC}}, \tag{1}$$

124
$$[POA] = \frac{\sum_{i}[tr_{i}]}{f_{POA}},$$
 (2)

$$[SOC] = \frac{\sum_{i} [tr_i]}{f_{SOC}}, \tag{3}$$

$$[SOA] = \frac{\sum_{i} [tr_i]}{f_{SOA}}, \tag{4}$$

where Σ i[tri] is the total concentration of the selected tracers in the sample, denoting representative compounds from specific emission categories; f_{POC} and f_{POA} are the mass fractions of the tracers in OC and PM_{2.5} from primary emissions, respectively. Similarly, f_{SOC} and f_{SOA} are the mass fractions of the tracers in OC and PM_{2.5} from secondary emissions, respectively. The calculated [POC], [POA], [SOC], and [SOA] are the contributions of different primary and secondary sources to OC and PM_{2.5}. Here, we identified mass fractions

for representative tracers from several significant primary and secondary emission sources. The primary sources included biomass burning, coal combustion, vehicle exhaust, cooking activities, plant debris, and fungal spores. The secondary sources were categorized into biogenic (isoprene, monoterpenes, and sesquiterpenes) and anthropogenic (toluene and naphthalene) sources. Table S2 presents information on the representative tracers, their corresponding f_{OC} and f_{OA} , and relevant references.

132

133

134

135

136

137

138

139

140

141

142

143

144

145

146

147

148

149

150

151

152

153

154

155

156

157

158

We employed the CMB model (version 8.2) provided by the US Environmental Protection Agency to verify the results calculated using a tracer-based method. This model assumes a CMB between the emission sources and environmental receptors. Thus, the mass of pollutants is not lost during transport from the source to the receptor, and the measured chemical component concentration at the receptor is the linear superposition of the contribution of each source class to the concentration (Stone et al., 2009). The CMB model operates on principles analogous to those involved in the tracer-based method, relying on the mass fractions of characteristic tracers in OC and OAs from emission sources to ascertain the contributions of different sources. Thus, theoretically, the results generated by the CMB model should be consistent with those obtained from the tracer-based method. The tracer-based method and CMB model inherently involve a degree of uncertainty, primarily owing to variability in the mass fractions of representative tracers in OC and OA (f_{oc} and f_{oa}) from the same emission source across different observational studies (Ding et al., 2012 and 2014). For instance, levoglucosan—a molecular marker for biomass burning—has been found to represent varying proportions of OC in different studies. Andreae et al. (2009) reported a levoglucosan-to-OC ratio (f_{oc}) of approximately 0.1186, with Zheng et al. (2002) observing a higher average value of 0.1258, and Zhang et al. (2007) reported a lower f_{oc} value of 0.082 for biomass burning emissions. Nevertheless, this method has been widely employed to estimate the contributions of various primary and secondary sources to OC and aerosols, yielding relatively reasonable results (Kleindienst et al., 2007 and 2012; Stone et al., 2009; Ding et al., 2012 and 2014; Al-Naiema et al., 2017; Ren et al., 2021; Xu et al., 2021; Haque et al., 2023). To further reduce uncertainty, additional observational studies are essential for identifying representative tracers in emission sources and determining their mass fractions in OC and OA (Oros and Simoneit, 2000; He et al., 2004; Zhao et al., 2007; Zhang et al., 2008; Kleindienst et al., 2012; Andreae, 2019).

Furthermore, we employed the EC-based method to estimate the total POC and SOC concentrations,

enabling a comparison with the POC and SOC concentrations obtained using the tracer-based method. This
method uses EC as a tracer for POC and approximates the observed minimum ratio of OC to EC (OC/EC)_{min} as
an equivalent to the primary emission OC/EC value (OC/EC)_{pri} (Turpin and Huntzicker, 1995; Castro et al.,
1999). The equation used for estimating SOC is

$$SOC_{EC-based} = OC - EC \times (OC/EC)_{min},$$
 (5)

- where the minimum OC/EC values observed in spring, summer, autumn, and winter were 2.01, 2.20, 2.15, and
- 165 2.31, respectively.

166

167

168

169

170

171

172

173

174

175

176

177

178

179

180

181

182

183

184

185

3 Results and discussion

3.1 Carbonaceous components

The OC and EC concentrations were in ranges of 1.01-13.66 (mean: $5.88 \pm 2.57 \,\mu g \, m^{-3}$) and $0.27-4.55 \,\mu g \, m^{-3}$ (mean: $1.75 \pm 0.88 \, \mu g \, m^{-3}$), respectively. Seasonal variations in the OC and EC concentrations closely mirrored those observed for PM_{2.5}, with elevated levels in autumn and winter and diminished levels in spring and summer (Figure 1a). The OC/EC ratio is a widely employed metric for characterizing emissions from fossil fuels and biomass combustion. OC/EC values below 1.1 typically indicate vehicle exhaust emissions; values within a range of 2-3 suggest coal combustion emissions, and values above 7 indicate biomass burning (Saarikoski et al., 2008). Here, the OC/EC range was 2.01-16.95, with the average value being 3.86 ± 2.05 . These OC/EC ratios fell within the ranges associated with coal and biomass burning emissions. This suggests that the carbonaceous material was predominantly derived from combustion. Furthermore, owing to its stability and resistance to chemical transformations in the atmosphere, EC is frequently employed as a tracer for primary emissions. The OC/EC ratio is a useful tool for assessing the relative contributions of primary and secondary sources (Castro et al., 1999; Turpin and Huntzicker, 1995). Generally, an OC/EC value above 2 indicates a predominant contribution of secondary sources to OC, whereas values below 2 suggest greater contributions from primary sources (Kunwar and Kawamura, 2014). Here, the majority of the OC/EC values exceeded 2 (Figure 1b), implying that the OC may have been significantly influenced by secondary sources. The OC/EC values were relatively high in summer (4.33 ± 2.07) and winter (4.18 ± 2.57) compared with those observed in spring (3.36 ± 1.98) and autumn (3.59 ± 1.22) . This indicates an increased contribution to OC from secondary sources during the summer and winter.

3.2 Major polar components

3.2.1 Fatty acids

186

187

188

189

190

191

192

193

194

195

196

197

198

199

200

201

202

203

204

205

206

207

208

209

210

211

212

A range of homologous straight-chain C10:0-C32:0 fatty acids (FAs) and unsaturated C16:1 and C18:1 FAs were detected in the PM_{2.5} samples (Figures 1c and 2a). Their distribution exhibited a strong even-carbonnumber predominance, as indicated by a carbon preference index (CPI) of 7.59 ± 7.42 (Figure S3a), with peaks at C16:0 and C18:0. The total FA concentration was in a range of 3.24-657.86 ng m⁻³, with an average concentration of 196.50 ± 110.92 ng m⁻³. Similar molecular distribution patterns and concentrations have been documented in urban aerosol studies across China (59-2,090 ng m⁻³; He et al., 2004 and 2006; Wang et al., 2006; Haque et al., 2019; Fan et al., 2020). In these Chinese cities, FAs are primarily influenced by biogenic sources, including plant releases and biomass burning, as well as fossil fuel combustion and residential cooking. This average concentration generally exceeds those observed for coastal and marine aerosol samples (0.1–160 ng m⁻³; Kawamura et al., 2003; Wang et al., 2007; Fu et al., 2011), which are primarily influenced by marine biological activities and long-range transport of continental sources. High-molecular-weight FAs (HFAs, ≥ C20:0) are typically derived from the waxes of terrestrial higher plants or biomass burning, whereas low-molecular-weight FAs (LFAs, < C20:0) originate from more diverse sources, including vascular plants, microorganisms, marine phytoplankton, and kitchen emissions (Fu et al., 2008 and 2010). Consequently, the ratio of LFAs to HFAs (LFA/HFA ratio) is an indicator of the relative contributions from various sources. Here, the LFA/HFA range was 0.34-10.67, with an average of 2.45 ± 1.53 (Figure S3b), suggesting that the FAs may have originated from a mixture of natural and anthropogenic sources. The specific FAs C16:0 and C18:0 are associated with different sources. C16:0 is primarily derived from biomass burning or plant emissions, whereas C18:0 predominantly originates from vehicle exhaust, cooking emissions, or road dust (Wang et al., 2007; Fu et al., 2010). Thus, the ratio of C18:0 to C16:0 (C18:0/C16:0) is frequently employed to assess the FA source. A C18:0/C16:0 ratio below 0.25 suggests a primary contribution from biomass burning or plant emissions, whereas ratios between 0.25 and 0.5 indicate a predominant influence from vehicle exhaust. C18:0/C16:0 ratios within a range of 0.5-1 suggest a significant contribution from cooking emissions or road dust (Rogge et al., 2006). Here, the C18:0/C16:0 ratio varied from 0.05 to 9.53, with an average value of 0.59 \pm 0.88 (Figure S3c), indicating that the FAs in Nanchang originated from a mixture of sources.

The average concentrations of unsaturated FAs, specifically C16:1 and C18:1, were 6.94 ± 4.35 and 3.79 ± 2.86 ng m⁻³, respectively. Such unsaturated FAs are primarily derived from biomass burning, plant leaf emissions, cooking activities, and release from marine organisms (Kawamura and Gagosian, 1987; Rogge et al., 1993; Nolte et al., 1999). Upon emission into the atmosphere, unsaturated FAs undergo rapid oxidation by ozone (O₃), hydrogen peroxide (H₂O₂), or hydroxyl (OH) radicals. Consequently, the ratio of unsaturated FAs to saturated FAs, represented as (C16:1 + C18:1)/(C16:0 + C18:0), is an indicator of the reactivity and degree of aging of unsaturated FAs (Rudich et al., 2007; Kawamura and Gagosian, 1987). Here, this ratio was 0.12 \pm 0.06 (Figure S3d), indicating that the unsaturated FAs underwent significant photochemical degradation and that secondary organic compounds may be common in PM_{2.5}.

The average concentrations of most FAs were significantly (p < 0.05) higher in autumn and winter than in spring and summer (Figure 2a), indicating a substantial increase in fatty acid emissions during autumn and winter. The LFA/HFA and C18:0/C16:0 ratios were lower in autumn and winter than in summer (Figures S3b and S3c). This indicated that in autumn and winter, FAs were significantly influenced by terrestrial plant or biomass burning, whereas in summer, they were more influenced by vehicular emissions, marine phytoplankton, and cooking emissions. Conversely, the (C16:1 + C18:1)/(C16:0 + C18:0) values were higher in winter than in summer (Figure S3d). This suggested that unsaturated FAs experienced a greater degree of photochemical degradation during the warm seasons. Unsaturated FAs can be rapidly oxidized by ozone or OH radicals. The higher temperatures, relatively stronger solar radiation, and higher concentrations of O₃ and OH radicals in the summer season will facilitate the oxidative decomposition of unsaturated FAs (Wang et al.,

232 2006; Fan et al., 2020).

3.2.2 Fatty alcohols

Several straight-chain n-alkanols (C14–C32) were detected (Figures 1c and 2b), exhibiting a predominance of even carbon numbers, as indicated by a CPI of 10.28 ± 17.05 (Figure S3e). Low-molecular-weight alcohols (LMW_{alc}, \leq C20) exhibited peaks at C16 and C18, and high-MW alcohols (HMW_{alc}, \geq C20) exhibited peaks at C26, C28, and C30 (Figure 2b). The total concentration of n-alkanols was in a range of 5.80–572.01 ng m⁻³ (average = 113.99 ± 92.50 ng m⁻³). This concentration fell within the range of reported n-alkanol concentrations in urban aerosols in China (3.1–1,301.0 ng m⁻³; Wang et al., 2006; Haque et al., 2019; Fan et

al., 2020) and generally exceeded that of coastal and marine aerosol samples (0.1–19.7 ng m⁻³; Kawamura et al., 2003; Fu et al., 2011). In urban aerosols of China, fatty alcohols are primarily derived from vegetation releases, biomass burning, and resuspension of soil particles. The fatty alcohols in coastal and marine aerosols are primarily attributed to the long-range transport of terrestrial soil and biomass burning as well as marine biogenic sources. HMW_{alc} primarily originates from higher plant leaf waxes, loess deposits, or biomass burning, and LMW_{alc} primarily originates from soil and marine microorganisms (Simoneit, 2002; Kawamura et al., 2003). Here, the LMW_{alc} concentration (75.12 \pm 61.28 ng m⁻³) exceeded that of HMW_{alc} (39.09 \pm 34.07 ng m⁻³), yielding an average LMW/HMW ratio of 2.50 \pm 1.73 (Figure S3f), indicating a mixture of n-alkanols from soil, marine organisms, and biomass burning.

The average concentrations of most fatty alcohols were significantly (p < 0.05) higher in autumn and winter than in summer (Figure 2b), indicating a substantial increase in fatty alcohols emissions during autumn and winter. The LMW/HMW values were relatively low in autumn and winter and higher in spring and summer (Figure S3f). This suggests an increased contribution of soil and marine organisms to n-alkanols in spring and summer. Contributions from plant or biomass burning increased in autumn and winter. In Chinese cities, rising temperatures in spring increase soil microbial activity, with marine air masses exerting a stronger influence during summer, potentially increasing emissions from soil and marine organisms in these seasons. In contrast, autumn and winter coincide with the crop harvest and increased winter heating, leading to likely increases in biomass burning emissions during these periods (Wang et al., 2006; Haque et al., 2019; Fan et al., 2020).

3.2.3 Saccharides

We investigated three saccharide classes: anhydrosugars, primary sugars, and sugar alcohols. Among the anhydrosugars, levoglucosan had the highest concentration (102.48 ± 78.63 ng m⁻³). We observed markedly lower concentrations of mannosan (4.33 ± 4.04 ng m⁻³) and galactosan (2.41 ± 2.67 ng m⁻³) (Figure 2c). Levoglucosan—a prominent biomarker for biomass burning—has been extensively investigated in urban aerosol samples, with concentrations in a range of 22–2,706 ng m⁻³ (Wang and Kawamura, 2005; Wang et al., 2006; Fu et al., 2010; Haque et al., 2019; Fan et al., 2020), indicating the significant influence of biomass burning on the urban atmosphere. The widespread detection of levoglucosan in various environments—including suburban (10–482 ng m⁻³; Yttri et al., 2007; Fu et al., 2008), marine (0.2–30 ng m⁻³; Simoneit et al.,

2004a; Fu et al., 2011), and polar regions (0-3 ng m⁻³; Stohl et al., 2007; Fu et al., 2009)—indicates its potential for long-range atmospheric transport. Compared to those of the major polar organic compounds found in marine environments, such as FAs, fatty alcohols, and saccharides, the concentrations of these substances in urban PM_{2.5} are substantially higher. This is primarily attributed to the substantial impact of anthropogenic activities in urban environments—such as vehicle emissions, industrial processes, and residential heating and cooking—all of which can release these major polar components (Wang et al., 2006; Fu et al., 2008; Haque et al., 2019; Fan et al., 2020). In contrast, the organic matter in marine $PM_{2.5}$ originates from relatively simpler sources with lower emissions, mainly influenced by natural processes, including marine biological activity and the long-range transport of continental pollutants (Kawamura et al., 2003; Simoneit et al., 2004a; Wang et al., 2007; Fu et al., 2011). Seasonal variations of anhydrosugars exhibited consistent patterns, with elevated concentrations in autumn and winter and reduced levels in spring and summer (Figure 2c). This indicated increased biomass burning during the cold months. The sources were characterized using levoglucosan-to-mannosan (L/M) and mannosan-to-galactosan (M/G) ratios. Research suggests distinct L/M ranges for different biomass burning sources: softwood (3–10), hardwood (13–35), and agricultural crop burning (40–56) (Oros and Simoneit, 2001; Sheesley et al., 2003; Engling et al., 2014). Coal combustion can produce significant amounts of levoglucosan (Sheesley et al., 2003; Fabbri et al., 2009), typically with higher L/M values (12–189) because of the lower cellulose content compared with that of plant materials (Rybicki et al., 2020a and 2020b). Conversely, M/G values are generally higher for softwood and hardwood combustion at 3.6–7.0 and 1.2–2.0, respectively. However, M/G values are relatively low for agricultural crop burning (0.3-0.6) (Oros and Simoneit, 2001; Sheesley et al., 2003). Here, most samples exhibited relatively high L/M ratios (4.63–466.61, average = 40.22 \pm 49.82) and relatively low M/G ratios (0.30–9.41, average = 2.34 \pm 1.36). The L/M and M/G ratios were similar to those of previous observations in the urban area of Nanchang (L/M = 7.9–359.1; average = 59.9; Zhu et al., 2022) and fell within the ranges for crop residue burning and coal combustion. This suggests that the dehydrosugars in the PM_{2.5} of Nanchang were likely primarily derived from crop residue burning and coal combustion. In autumn and winter, the contributions of crop residue burning and coal combustion were more prominent, as evidenced by the higher L/M ratios and lower M/G ratios observed compared with those in

267

268

269

270

271

272

273

274

275

276

277

278

279

280

281

282

283

284

285

286

287

288

289

290

291

292

spring and summer (Figures S3g and S3h).

294

295

296

297

298

299

300

301

302

303

304

305

306

307

308

309

310

311

312

313

314

315

316

317

318

319

320

Primary sugars and sugar alcohols serve as tracers for primary biological aerosol particles, originating from biogenic emissions, including the release of microorganisms, plants, and flowers, as well as the resuspension of surface soils and unpaved road dust containing biological materials (Graham et al., 2003; Simoneit et al., 2004b; Yttri et al., 2007). Furthermore, biomass burning is a notable source of primary sugars and sugar alcohols (Fu et al., 2012). We identified nine primary sugars (ribose, fructose, galactose, glucose, sucrose, lactulose, maltose, turanose, and trehalose; Figure 2c). Glucose (14.90 \pm 6.62 ng m⁻³) and sucrose (14.68 \pm 6.48 ng m⁻³) exhibited the highest concentrations, followed by fructose (10.82 \pm 4.54 ng m⁻³), trehalose (7.92 \pm 4.40 ng m⁻³), and maltose (5.39 \pm 3.43 ng m⁻³). The concentrations of galactose (1.88 \pm 1.24 ng m⁻³), ribose $(2.87 \pm 2.18 \text{ ng m}^{-3})$, turanose $(0.87 \pm 0.61 \text{ ng m}^{-3})$, and lactulose $(0.83 \pm 0.54 \text{ ng m}^{-3})$ were comparatively low. We detected four sugar alcohols (mannitol, arabitol, pinitol, and inositol). Mannitol ($9.88 \pm 4.57 \text{ ng m}^{-3}$) exhibited the highest concentration, followed by pinitol $(6.05 \pm 4.23 \text{ ng m}^{-3})$ and arabitol $(4.96 \pm 3.39 \text{ ng m}^{-3})$. The concentration of inositol $(2.05 \pm 1.66 \text{ ng m}^{-3})$ was low. Levoglucosan serves as a specific biomarker for biomass burning, enabling the assessment of biomass burning contributions to sugar compounds through the ratio of levoglucosan to OC (Lev/OC) and the proportion of levoglucosan in the total sugar compounds (Lev%). Typically, a Lev/OC ratio of >0.048 and a Lev% of >68% indicate a dominance of biomass burning. Conversely, values below these thresholds suggest that in addition to biomass burning, other sources, such as biogenic emissions, significantly contribute to the presence of sugar compounds (Yan et al., 2019 and references therein). Here, the Lev% and Lev/OC values were $53.57\% \pm 17.93\%$ and 0.016 ± 0.009 (Figures S3i and S3j), respectively, indicating that the sugar compounds were influenced by biomass burning and biogenic emissions, particularly the primary sugars and sugar alcohols. Primary sugars, such as glucose and trehalose, as well as the mannitol in sugar alcohol, positively correlated with levoglucosan (Figure S4a). This confirmed that biomass burning may be a potential source of primary sugars and sugar alcohols. However, the correlation was not statistically significant, suggesting that biological sources remain an important contributor to these compounds in Nanchang. The Lev/OC and Lev% values were higher in autumn and winter than in spring and summer (Figures S3i and S3j), further indicating that biomass burning contributions increased during the cold months. As previously noted,

the primary reason for increased biomass burning emissions during the cold season is that autumn marks the crop harvest in China, leading to more straw burning. Furthermore, the temperature decrease in winter results in additional biomass burning for heating purposes.

3.3 Minor polar components

321

322

323

324

325

326

327

328

329

330

331

332

333

334

335

336

337

338

339

340

341

342

343

344

345

346

347

3.3.1 Lignin, resin products, and sterols

Here, we detected four types of lignin and resin-derived compounds: 4-hydroxybenzoic acid, dehydroabietic acid, vanillic acid, and syringic acid (Figures 1c and 3a). These are generally considered to originate from natural plant release and burning. The burning of coniferous trees, such as pine, releases higher concentrations of dehydroabietic acid than other lignin and resin-derived compounds (Simoneit, 2002). Here, the concentrations of 4-hydroxybenzoic acid (5.06 \pm 3.57 ng m⁻³) and dehydroabietic acid (2.98 \pm 1.91 ng m⁻³) were high, whereas those of vanillic acid (1.50 \pm 1.08 ng m⁻³) and syringic acid (1.53 \pm 1.11 ng m⁻³) were relatively low. A significant positive correlation was observed between the total concentration of lignin and resin-derived compounds and levoglucosan (r = 0.80, p < 0.01, Figure S4a), suggesting that biomass burning was a potential source of lignin and resin-derived compounds. The concentration of dehydroabietic acid was significantly lower than that of 4-hydroxybenzoic acid, similar to the pattern observed for Nanjing aerosols (Haque et al., 2019). This implies that coniferous tree combustion may not be the primary source of lignin and resin acids in this region. We identified several sterols (cholesterol, stigmasterol, and β -sitosterol; average concentrations = 4.63 \pm 3.17, 4.89 ± 3.68 , and 10.11 ± 8.26 ng m⁻³, respectively; Figure 3a). These sterols originate from distinct sources. Cholesterol, an animal-derived sterol, is primarily associated with meat cooking in the atmosphere (Rogge et al., 1991; Nolte et al., 1999; He et al., 2004). Contrarily, stigmasterol and β-sitosterol are plantderived sterols, typically originating from plant leaves, cooking, or biomass burning (Nolte et al., 2001; He et al., 2004; Zhao et al., 2007). Here, stigmasterol and β-sitosterol exhibited a significant positive correlation with levoglucosan (Figure S4a). This suggests that biomass burning may be a potential source of plant-derived sterols. The concentrations of stigmasterol and β-sitosterol were higher in autumn and winter than in spring and summer, indicating an increased contribution of biomass burning to sterols in autumn and winter.

3.3.2 Glycerol and hydroxy acids

Glycerol and three hydroxy acids, glycolic acid, malic acid, and citric acid, were detected in the PM_{2.5} samples (Figures 1c and 3b). The concentration of glycerol was relatively high $(9.99 \pm 4.13 \text{ ng m}^{-3})$, whereas the three hydroxy acids exhibited comparable and relatively low concentrations: glycolic acid (7.16 \pm 1.90 ng m⁻³), malic acid (6.60 \pm 1.85 ng m⁻³), and citric acid (5.92 \pm 1.99 ng m⁻³). These concentrations aligned with reported ranges for urban aerosols (2–146 and 1–180 ng m⁻³ for glycerol and hydroxy acids, respectively; Wang et al., 2006; Fu et al., 2010; Haque et al., 2019; Fan et al., 2020). The source of glycerol in urban aerosols is similar to that of sugar alcohols, primarily originating from the emission from plants, the resuspension of surface soils and unpaved road dust containing biological materials, and biomass burning (Simoneit et al., 2004a and 2004b; Fu et al., 2008), whereas glycolic, malic, and citric acids mainly originate from the secondary photooxidation of organic compounds in the atmosphere, such as biogenic unsaturated FAs, cyclic olefins, and isoprene (Kawamura and Ikushima, 1993; Kawamura and Sakaguchi, 1999; Claeys et al., 2004, Haque et al., 2019). No significant correlation was observed between glycerol and the hydroxy acids; however, a notable correlation was observed among the hydroxy acids (r = 0.49-0.66, p < 0.01, Figure S4b). This confirmed the divergent sources of glycerol and hydroxy acids and similar origins for the hydroxy acids. In summer, the concentrations of the hydroxy acids exceeded those in other seasons (Figure 3b). A positive correlation was observed between the polyacids and temperature (r = 0.35-0.51, p < 0.01), suggesting enhanced secondary photochemical oxidation in the warm months. The secondary formation of hydroxy acids in the atmosphere is suggested to be related to the ozone-driven oxidation of organic compounds. Elevated ozone levels and stronger solar radiation during the summer season create more favorable conditions for the secondary production of hydroxy acids (Kawamura and Ikushima, 1993; Kawamura and Sakaguchi, 1999; Claeys et al., 2004).

3.3.3 Aromatic acids

348

349

350

351

352

353

354

355

356

357

358

359

360

361

362

363

364

365

366

367

368

369

370

371

372

373

374

We detected four aromatic acids in the PM_{2.5} samples: benzoic acid, phthalic acid, isophthalic acid, and terephthalic acid at concentrations of 0.76 ± 0.34 , 6.40 ± 4.05 , 1.10 ± 0.74 , and 10.06 ± 3.07 ng m⁻³, respectively (Figure 3b). Aromatic acids significantly contribute to the formation of atmospheric particles. Benzoic acid is recognized as a major pollutant in vehicle exhaust and the secondary photochemical oxidation product of aromatic hydrocarbons from vehicle emissions (Kawamura and Kaplan, 1987; Rogge et al., 1993;

Kawamura et al., 2000). Phthalic acid typically originates from the secondary transformation of PAHs, including naphthalene and other PAHs. Terephthalic acid is primarily produced through terephthalate hydrolysis during the combustion of urban plastics (Fu et al., 2010; Haque et al., 2019). Here, phthalic and terephthalic acids jointly accounted for approximately 90% of the total detected aromatic acids. A significant positive correlation was observed between phthalic acid and PAHs (r = 83, p < 0.01), as well as between terephthalic acid and the total phthalates (r = 0.72, p < 0.01). The PAH and phthalate data have been published by Guo et al. (2024a and 2004b). This suggests that the secondary conversion of PAHs and the hydrolysis of phthalates (specifically terephthalate) during plastic burning significantly contribute to aromatic acid levels. The phthalic acid concentrations were higher in autumn and winter, whereas terephthalic acid levels peaked in spring and summer (Figure 3b). This indicates that the secondary transformation of PAHs was more pronounced during the cold months, whereas high temperatures in spring and summer promoted the volatilization and transformation of phthalates from plastic sources. Phthalates are employed as plasticizers in resins and polymers. Because they are not chemically bound to the polymer matrix, they can be easily released into the air through evaporation. Higher ambient temperatures in spring and summer favor phthalate release from the matrix (Wang et al., 2006; Fu et al., 2010).

390 3.4 SOA tracers in PM_{2.5}

3.4.1 Biogenic SOA tracers

Biogenic and anthropogenic SOAs are critical in influencing the atmospheric radiation balance and regional air quality (Ding et al., 2014). Biogenic SOA tracers include oxidation products from isoprene, monoterpenes, sesquiterpenes, and other oxygenated hydrocarbons. Isoprene is the dominant component of BVOC emissions, accounting for ~45% of the total emissions (annual release estimated at 600 Tg C) (Piccot et al., 1992; Guenther et al., 1995; Sharkey et al., 2008). Here, we detected six isoprene oxidation products (2-methylglyceric acid (2-MGA), three C5-alkene triols, and two 2-methyltetrols (MTLs) at concentrations of 1.83 ± 1.11 , 2.84 ± 1.88 , and 4.14 ± 3.27 ng m⁻³, respectively; Figure 4). The concentrations of the C5-alkene triols and MTLs exceeded that of 2-MGA. Generally, C5-alkene triols primarily originate from the secondary transformation of VOCs released during biomass burning and higher plant waxes (Fu et al., 2010 and 2014). Throughout the sampling period, a strong linear correlation was observed between the MTLs and C5-alkene

triols ($R^2 = 0.82$, P < 0.01), indicating their similar sources. Nevertheless, certain differences were observed in the formation processes of C5-alkene triols and MTLs. Both compounds are formed through the acid-catalyzed ring opening of isoprene epoxydiols (Surratt et al., 2006 and 2010); however, the formation of C5-alkene triols is enhanced in acidic aerosol environments (Yee et al., 2020). Here, the ratios of C5-alkene triols to MTLs (C5/MTLs) were elevated in autumn compared with those in summer (Figure S5a), suggesting that increased aerosol acidity in the cold months may facilitate the production of C5-alkene triols. C5-alkene triols and MTLs are believed to form via isoprene oxidation under low-NO_x conditions (Surratt et al., 2010; Lin et al., 2013). Contrarily, high concentrations of NO_x favor further isoprene oxidation to yield 2-MGA (Lin et al., 2013; Nguyen et al., 2015). Here, the 2-MGA/MTL ratios in winter exceeded those observed in other seasons (Figure S5b), indicating that elevated NO_x concentrations in winter (Figure S2) may enhance 2-MGA formation. In MTLs, 2-methylthreitol and 2-methylerythritol (MTL1 and MTL2) exhibited a significant linear correlation $(R^2 = 0.68, P < 0.01)$, indicating that they may originate from similar sources and/or share similar formation pathways. The ratio of MTL2 to MTLs (MTL2/MTL ratio) can reflect the transformation pathways of MTLs. The ratio of MTL2/MTLs = 0.35, 0.61, 0.76, and 0.90 corresponded to isoprene secondary transformation from biogenic sources, OH-rich conditions (low NO_x), NO_x-rich conditions, and liquid-phase oxidation by H₂O₂, respectively (Kleindienst et al., 2009; Nozière et al., 2011). The results showed that the MTL2/MTL values in spring (0.64 ± 0.12) and summer (0.59 ± 0.11) were relatively low and closer to the values for biogenic sources and OH-rich secondary transformation. However, the values in autumn and (0.66 ± 0.10) winter (0.69 ± 0.06) were relatively high, approaching those for NO_x-rich secondary transformation and liquid-phase oxidation by H₂O₂ (Figure S5c). This indicates that in spring and summer, MTLs were more likely derived from biogenic sources and OH-rich secondary transformation, whereas in autumn and winter, a shift was observed toward NO_x-rich secondary transformations and liquid-phase oxidation by H₂O₂. This relatively high C5/MTL, 2-MGA/MTL, or MTL2/MTL ratio observed during the cold season compared to that in the warm season is commonly reported in urban environments across China, including Beijing (Liu et al., 2023), Tianjin (Wang et al., 2019; Fan et al., 2019), Nanjing (Yang et al., 2022), Shanghai (Yang et al., 2022), and Guangzhou (Yuan et al., 2018). This phenomenon is primarily attributed to higher NO_x concentrations and increased aerosol acidity in the cold season versus the warm season in Chinese cities, which promote the formation of secondary C5-

402

403

404

405

406

407

408

409

410

411

412

413

414

415

416

417

418

419

420

421

422

423

424

425

426

427

alkene triols, 2-MGA, and MTL2.

429

430

431

432

433

434

435

436

437

438

439

440

441

442

443

444

445

446

447

448

449

450

451

452

453

454

455

Monoterpenes represent a crucial component of BVOC emissions, accounting for ~11% of the annual emissions, with an annual emission of 110 Tg C (Guenther et al., 1995). Here, we identified four oxidation products of monoterpene (pinonic acid (PNA); pinic acid (PA); 3-methyl-1,2,3-butanetricarboxylic acid (MBTCA); and 3-hydroxyglutaric acid (3-HGA) at concentrations of 1.69 ± 0.99 , 1.47 ± 0.86 , 0.79 ± 0.61 , and 0.77 ± 0.52 ng m⁻³, respectively (Figure 4). The concentrations of PNA and PA exceeded those of MBTCA and 3-HGA. PNA and PA are produced via the oxidation of α/β -pinene via reactions with O_3 and OH radicals, and the α/β -pinene detected in the aerosol samples is primarily derived from biomass burning and higher plant release (Hallquist et al., 2009; Eddingsaas et al., 2012; Zhang et al., 2015; Iyer et al., 2021). The predominance of PNA over PA is attributable to its relatively high vapor pressure, consistent with previous findings (Fu et al., 2008 and 2010). PNA and PA are recognized as first-generation oxidation products of α-/β-pinene, whereas MBTCA represents a second-generation oxidation product formed via the further photooxidation of PNA and PA with OH radicals. The relative concentrations of such first- and second-generation oxidation products (M/P) reflect the oxidation degree and aging status of monoterpene compounds (Ding et al., 2014). Here, the M/P values were higher in spring (0.25 ± 0.11) and summer (0.32 ± 0.10) than in autumn (0.16 ± 0.09) and winter (0.24 \pm 0.10). This suggests that higher temperatures and/or stronger radiation in spring and summer promoted the oxidation of monoterpene compounds (Figure S5d). The formation of 3-HGA is considered to occur via a ring-opening mechanism, probably linked to heterogeneous reactions of monoterpenes with irradiation in NO_x-rich environments (Jaoui et al., 2005; Claevs et al., 2007). The ratio of MBTCA to 3-HGA (MBTCA/3-HGA) can be employed to distinguish monoterpenes as the secondary transformation of α-pinene yields MBTCA at significantly higher rates relative to 3-HGA compared with β-pinene (Jaoui et al., 2005). Here, the annual MBTCA/3-HGA value was 1.18 ± 0.65 (Figure S5e), close to those observed in urban environments in the United States (0.81 \pm 0.32) and other cities in China (0.68 \pm 0.65) (Lewandowski et al., 2013; Ding et al., 2014). This suggests that monoterpenes in these urban environments have similar sources. The MBTCA/3-HGA value was higher in spring (1.31 ± 0.66) and summer (1.45 ± 0.70) than in autumn (1.09) \pm 0.72) and winter (0.88 \pm 0.32) (Figure S5e). This suggests that the contribution of α -pinene to monoterpene was higher in spring and summer than in autumn and winter. This phenomenon can be attributed to the

association of 3-HGA formation with NO_x-rich environments, where the relatively high NO_x concentrations in autumn and winter (Figure S2) may enhance 3-HGA production. The ratio of the total isoprene to monoterpene oxidation products (Iso/Pine) was lower in autumn and winter than in summer (Figure S5f). This pattern is also commonly observed in other urban environments of China, suggesting that the higher temperatures in summer favored isoprene release (Li et al., 2018; Fan et al., 2020; Liu et al., 2023).

BVOC emissions include a class of sesquiterpene compounds, among which β-caryophyllene is the most abundant and frequently reported (Ding et al., 2014; Fan et al., 2020). β-caryophyllinic acid, a product of the ozonolysis or photooxidation of β-caryophyllene, predominantly originates from biomass burning and natural plant emissions, including those from pine and birch trees (Helmig et al., 2006; Duhl et al., 2008). Here, β-caryophyllinic acid was detected at a concentration of 2.74 ± 1.92 ng m⁻³. The β-caryophyllinic acid concentrations in autumn (3.16 ± 1.77 ng m⁻³) and winter (4.63 ± 1.61 ng m⁻³) exceeded those observed in spring (1.49 ± 0.68 ng m⁻³) and summer (1.14 ± 0.47 ng m⁻³) (Figure 4). The higher concentrations of caryophyllinic acid in autumn and winter may be associated with increased biomass burning and subsequent secondary transformation of β-caryophyllene. During the sampling period, a significant positive linear correlation was observed between β-caryophyllinic acid and levoglucosan, supporting this inference (R² = 0.66, P < 0.01).

3.4.2 Anthropogenic SOA tracers

Anthropogenic SOA tracers include hydroxy and aromatic acids, which primarily originate from the secondary transformation of AVOCs. Although global AVOC emissions are relatively modest at 110 Tg C yr⁻¹ (Piccot et al., 1992) compared with BVOC emissions, which reach 1,150 Tg C yr⁻¹ (Guenther et al., 1995), the contribution of anthropogenic sources to SOA is frequently more pronounced in urban environments because of the impact of human activities (von Schneidemesser et al., 2010; Ding et al., 2012; Li et al., 2019). AVOC emissions in urban settings can enhance BVOC oxidation, promoting SOA formation (Carlton et al., 2010; Hoyle et al., 2011). Here, we identified two primary anthropogenic SOA tracers, 2,3-dihydroxy-4-oxopentanoic acid (DHOPA) and phthalic acid, at concentrations of 1.73 ± 1.10 and 6.38 ± 4.05 ng m⁻³, respectively (Figures 3 and 4). DHOPA and phthalic acid are recognized as important markers for anthropogenic SOAs, produced via the oxidation of toluene and PAHs, such as naphthalene (Kawamura and

Ikushima, 1993; Kleindienst et al., 2007 and 2012). Their concentrations were higher in autumn and winter than in spring and summer (Figures 3 and 4). This indicated a marked increase in the contribution of anthropogenic sources to SOA during the cold months. As typical anthropogenic SOA tracers, DHOPA and phthalic acid have been reported to exhibit significantly higher concentrations in urban areas than in suburban and remote regions, with higher levels in the cold season than in the warm season in China (Ding et al., 2014; Fan et al., 2019; Yang et al., 2022). SOAs in urban environments and in the cold season in China are more strongly influenced by anthropogenic emissions, such as those from fossil fuel combustion and biomass burning (Ding et al., 2012; Yuan et al., 2018; Fan et al., 2019).

3.5 Source apportionment of organic carbon and aerosol

483

484

485

486

487

488

489

490

491

492

493

494

495

496

497

498

499

500

501

502

503

504

505

506

507

508

509

Employing a tracer-based methodology, we quantified the contributions of POC and SOC to the total OC (Figure 5). The results showed that the POC and SOC concentrations were 3.22 ± 1.81 and 0.50 ± 0.32 µg m⁻³ (Figures 5a-5c), accounting for $53.30\% \pm 12.53\%$ and $8.33\% \pm 3.29\%$ of the measured OC, respectively (Figure 5f). Our results indicate that POC continues to be the main contributor to OC. The higher proportion of POC is likely attributed to the greater diversity and higher concentrations of primarily emitted organic compounds identified in our study, whereas secondary organic compounds showed fewer species and lower concentrations. These results were within the reported ranges of POC (5%-76%) and SOC (3%-56%) (Stone et al., 2009; Guo et al., 2012; Fan et al., 2020; Xu et al., 2021; Haque et al., 2023). Notably, anthropogenic sources, including biomass burning, coal combustion, motor vehicle emissions, and cooking, contributed the majority of POC (2.89 \pm 1.72 µg m⁻³, accounting for 88.98% \pm 6.24%). Natural sources, such as plant debris and fungal spores, contributed relatively little (0.33 \pm 0.17 μg m⁻³, accounting for 11.01% \pm 6.24%). For SOC, anthropogenic contributions (0.33 \pm 0.25 μg m⁻³, accounting for 60.67% \pm 21.29%), including toluene and naphthalene, exceeded biogenic contributions (0.17 \pm 0.09 μ g m⁻³, accounting for 39.05% \pm 21.15%), which included isoprene, α/β -pinene, and β -caryophyllene. The relative abundances of anthropogenic POC and SOC were higher in autumn and winter, whereas biogenic POC and SOC exhibited greater relative abundances during spring and summer (Figures 5d-5f). These results underscore the significant influence of biogenic emissions during the warm months, whereas anthropogenic emissions exert a pronounced effect during the cold months. This situation is primarily attributed to the elevated temperatures, and increased solar radiation

during the warm months facilitates VOC release from vegetation, thereby promoting biogenic POC emissions and SOC formation. Contrarily, the rise in anthropogenic POC emissions from biomass burning and coal combustion during the cold months fosters the development of anthropogenic SOC in the atmosphere. During winter, including both pollution episodes (Winter-P) and the remainder period (Winter-R), the contribution proportions of two anthropogenic POC sources (biomass and coal combustion, 34%–36%) and anthropogenic SOC precursors (toluene and naphthalene, 6%–7%) were consistently higher than the annual averages (27% for these two anthropogenic POC and 5% for anthropogenic SOC) (Figure 5f). This trend was even more pronounced during individual pollution episodes (Figure S6), with anthropogenic POC contributions reaching 31%-42% and anthropogenic SOC contributions increasing to 6%-9% (Figure S6f). These findings suggest that POC from coal and biomass combustion, along with SOC originating from toluene and naphthalene, may be key drivers of wintertime organic aerosol pollution. Although the contribution of SOC to OC is substantially smaller than that of POC, the impact of SOC should not be overlooked. First, this study identified only five types of SOC products, and there may be other SOC products—such as liquid-phase SOC products and primary aging SOC products—that cannot be effectively detected using the SOC tracer method (Ding et al., 2014). Therefore, the SOC contribution estimated by the SOC tracer method is likely underestimated. Second, numerous studies have demonstrated that even a small increase in the proportion of SOC during winter pollution periods can worsen OA pollution (Li et al., 2019; Xu et al., 2021; Haque et al., 2023). Similarly, using a tracer-based method, we quantified the contributions of POA and SOA to PM_{2.5} (Figure S7). The findings indicated that POA and SOA contributed 6.13 ± 3.58 and 1.02 ± 0.63 µg m⁻³, accounting for $21.02\% \pm 6.50\%$ and $3.47\% \pm 1.41\%$ of the observed PM_{2.5} mass in Nanchang, respectively. The anthropogenic POA (5.50 \pm 3.41 μ g m⁻³, accounting for 88.74% \pm 6.46%) and SOA (0.65 \pm 0.48 μ g m⁻³, accounting for $58.79\% \pm 21.30\%$) exceeded the natural POA ($0.63 \pm 0.33 \,\mu g \,m^{-3}$, accounting for $11.26\% \pm 0.33 \,\mu g \,m^{-3}$ 6.46%) and SOA (0.37 \pm 0.20 μg m⁻³, accounting for 40.93% \pm 21.19%), respectively. The POA and SOA exhibited patterns analogous to those of POC and SOC, with greater contributions recorded in autumn and winter compared with spring and summer. We also employed the CMB model to calculate the contributions of different sources of POC and SOC to OC. The results derived from the CMB approach were largely consistent with those obtained using the tracer-

510

511

512

513

514

515

516

517

518

519

520

521

522

523

524

525

526

527

528

529

530

531

532

533

534

535

based method (Figure S8). The present results confirmed that both methods exhibited similar reliabilities. We employed the EC-based method to estimate the total POC and SOC concentrations. Dissimilar to the tracer-based method, which quantifies partial POC and SOC concentrations from specific sources, the EC-based method simply partitions the OC into POC and SOC, which calculates the total POC and SOC concentrations. The results demonstrated that the overall trends of the total POC and SOC calculated by the EC-based method were consistent with those obtained via the tracer-based method (Figure S9).

3.6 Characteristics of OAs during winter pollution

From an annual timescale perspective, anthropogenic POC and SOC are synchronous with the measured OC and observed PM_{2.5} mass (Figure S9). Correlation analysis revealed that anthropogenic POC and SOC exhibited a significant positive correlation (r = 0.72–0.80, P < 0.01) with the measured OC (Figure 6a). Redundancy analysis revealed that anthropogenic POC and SOC significantly contributed (40%–65%, P < 0.01) to the variations in OC concentration (Figure 6a). This suggests that anthropogenic OC and SOC are important factors influencing changes in the OC and PM_{2.5} mass throughout the sampling period. Variations in POC, SOC, OC, and PM_{2.5} mass were associated with specific meteorological conditions and gaseous pollutant concentrations. For instance, high POC, SOC, OC, and PM_{2.5} concentrations corresponded to elevated atmospheric pressure, reduced precipitation, and increased NO₂ concentrations (Figure S2). This suggests that meteorological conditions and gaseous pollutant concentrations could also influence POC, SOC, OC, and PM_{2.5} mass.

However, winter presents a different scenario. Regardless of whether it is during the winter pollution periods or other times in winter, POC did not maintain good consistency with the changes in the total OC content and $PM_{2.5}$ mass, whereas SOC remained synchronized with their variations (Figure S9). This phenomenon is particularly pronounced during individual pollution episodes in winter (Figure S9). Correlation and redundancy analyses further revealed that source-specific SOC, derived using the tracer methods, and the total SOC, calculated using the EC-based method, exhibited significant positive correlations with the measured OC (r > 0.6, P < 0.05) and significantly contributed (> 40%, P < 0.05) to their variations in entire winter pollution periods and individual pollution episodes (Figures 6b and 6d–6l). Given the relatively small number of nonpolluted days in winter and their scattered distribution across different dates, the correlations and

contribution levels were not as evident during the remainder of the winter season (Figures 6c). These findings indicate that on shorter timescales, particularly during brief PM pollution episodes lasting several days, SOC was a critical factor influencing the total OC content and PM_{2.5} mass.

The increased SOC concentration may be associated with elevated temperatures and NO_x concentrations during winter pollution episodes. This inference was supported by a significant linear positive correlation between temperature, NO₂ concentrations, and SOC concentrations observed during entire winter pollution periods and individual pollution episodes (Figures 7b and 7d-7l). An increase in short-term solar radiation intensity and oxidant levels have been shown to accelerate SOC formation (Fry et al., 2009; Ng et al., 2017; Li et al., 2018; Ren et al., 2019). Nevertheless, the contribution of POC should not be underestimated as its levels remained relatively high throughout the winter. This elevated POC concentration can also promote SOC transformation (Weber et al., 2007; Carlton et al., 2010; Hoyle et al., 2011; Srivastava et al., 2022). Although a negative correlation between temperature and SOC concentrations is observed on an annual timescale (Figure 7a), high NO₂ levels are also associated with high SOC concentrations over longer periods. The negative correlation between temperature and SOC concentrations on an annual scale mainly arises because emission sources and SOC transformation products decrease during warmer seasons, whereas they increase in colder seasons, especially winter (Haque et al., 2019; Fan et al., 2020). Outside pollution periods in winter, variations in temperature and NO₂ concentrations are minimal, which limits their promoting effect on SOC concentration increases (Figure 7c). Additionally, we analyzed the linear correlations between other meteorological factors and SOC. In particular, we examined the relations between wind speed, relative humidity, and SOC (Figure S10). The results indicated that no clear relation existed between wind speed and SOC. Although relative humidity showed some linear association with SOC during a few isolated pollution episodes, this relation was weak, with relatively large P-values and lacking statistical significance. These findings suggest that temperature and NO₂ concentrations are likely the main meteorological and oxidative factors driving the increase of SOC during winter pollution periods in the Nanchang region.

4 Conclusions

564

565

566

567

568

569

570

571

572

573

574

575

576

577

578

579

580

581

582

583

584

585

586

587

588

589

590

We investigated the composition and concentration of major polar organic compounds in PM_{2.5} samples collected over a year in Nanchang, Central China. The results revealed relatively high concentrations of FAs,

fatty alcohols, and saccharides, whereas lignin, resin products, sterols, glycerol, hydroxy acids, and aromatic acids were detected at low levels.

The study findings indicate that the organic components in the PM_{2.5} of Nanchang are predominantly derived from anthropogenic and natural sources. Anthropogenic sources were the primary contributors to OC and OA, and primary sources contributed more than secondary sources. Throughout the sampling period, we observed that the anthropogenic contributions significantly increased during autumn and winter, whereas biogenic contributions increased in spring and summer.

This study highlights the critical role of anthropogenic POC and SOC in influencing atmospheric PM_{2.5} pollution over an annual sampling period. During short-term pollution episodes in winter (lasting several days), the rapid secondary transformation emerged as the primary driver of OC increment and PM_{2.5} pollution. Elevated primary emissions and favorable oxidation conditions, such as increased light intensity and NO_x levels, were identified as key factors facilitating the rapid secondary transformation of OC during the winter pollution episodes.

The study findings underscore the necessity for targeted management strategies that consider primary and secondary anthropogenic emission sources across different seasons and pollution periods. Although the tracer-based method provided preliminary insights into the OC and OA from diverse sources, the study encountered inherent limitations in characteristic compound identification. The source apportionment analysis potentially underestimated contributions from unidentified primary and secondary sources because of the restricted range of tracers used. To address this, future research should prioritize comprehensive observational studies aimed at identifying representative molecular tracers across a broader spectrum of emissions and quantifying the precise mass fractions of such tracers in OC and OAs.

Data availability. The dataset associated with this paper is available upon request from the corresponding author (xiaohuayun@sjtu.edu.cn).

Competing interests. The authors declare that they have no conflict of interest.

- 618 **Author contributions.** Huayun Xiao conceptualized and designed the research. Sampling was conducted by
- 619 Zicong Li, and laboratory analyses were conducted by Wei Guo, Zicong Li, and Renguo Zhu. Data
- 620 interpretation was supported by Zhongkui Zhou and Hongwei Xiao. The manuscript was primarily written by
- Wei Guo, with contributions and consultations from all other authors.

- 623 Acknowledgements. We thank Ziyue Zhang and Liqin Cheng for their help with sampling and laboratory
- 624 work. This study was supported by the National Natural Science Foundation of China (grant number
- 41863002); the Jiangxi Provincial Natural Science Foundation (grant number 20242BAB25193); the Open
- 626 Foundation of Jiangxi Province Key Laboratory of the Causes and Control of Atmospheric Pollution, East
- 627 China University of Technology (grant number AE2209); and the Open Foundation of Yunnan Province Key
- 628 Laboratory of Earth System Science, Yunnan University (grant number ESS2024002).

629

630

References

- 631 Al-Naiema, I. M., and Stone, E. A.: Evaluation of anthropogenic secondary organic aerosol tracers from
- aromatic hydrocarbons, Atmos. Chem. Phys., 17, 2053–2065, https://doi.org/10.5194/acp-17-2053-2017,
- 633 2017.
- 634 An, Z. S., Huang, R. J., Zhang, R. Y., Tie, X. X., Li, G. H., Cao, J. J., Zhou, W. J., Shi, Z. G., Han, Y. M., Gu,
- Z. L., and Ji, Y. M.: Severe haze in northern China: A synergy of anthropogenic emissions and atmospheric
- processes, Proc. Natl. Acad. Sci. U.S.A., 116, 8657–8666, https://doi.org/10.1073/pnas.1900125116, 2019.
- Andreae, M. O.: Emission of trace gases and aerosols from biomass burning an updated assessment, Atmos.
- 638 Chem. Phys., 19, 8523–8546, https://doi.org/10.5194/acp-19-8523-2019, 2019.
- 639 Cao, J. J., and Cui, L.: Current Status, Characteristics and Causes of Particulate Air Pollution in the Fenwei
- 640 Plain, China: A Review, J. Geophys.Res-Atmos., 126, e2020JD034472,
- 641 https://doi.org/10.1029/2020JD034472, 2021.
- 642 Cao, J. J, Xu, H. M, Xu, Q., Chen, B. H., and Kan, H. D.: Fine particulate matter constituents and
- cardiopulmonary mortality in a heavily polluted Chinese city, Environ. Health Perspect., 120, 373–378,
- 644 https://doi.org/10.1289/ehp.1103671, 2012.
- 645 Carlton, A. G., Pinder, R. W., Bhave, P. V., and Pouliot, G. A.: To What Extent Can Biogenic SOA be
- 646 Controlled?, Environ. Sci. Technol., 44, 3376–3380, https://doi.org/10.1021/es903506b, 2010.

- 647 Castro, L. M., Pio, C. A., Harrison, R. M., and Smith, D. J. T.: Carbonaceous aerosol in urban and rural
- European atmospheres: estimation of secondary organic carbon concentrations, Atmos. Environ., 33, 2771–
- 649 2781, https://doi.org/10.1016/S1352-2310(98)00331-8, 1999.
- 650 Chen, C. R., Zhang, H. X., Yan, W. J., Wu, N. N., Zhang, Q., and He, K. B.: Aerosol water content
- enhancement leads to changes in the major formation mechanisms of nitrate and secondary organic aerosols
- in winter over the North China Plain, Environ. Pollut., 287, 117625,
- 653 https://doi.org/10.1016/j.envpol.2021.117625, 2021.
- 654 Cheng, Y. B., Ma, Y. Q., and Hu, D.: Tracer-based source apportioning of atmospheric organic carbon and the
- influence of anthropogenic emissions on secondary organic aerosol formation in Hong Kong, Atmos. Chem.
- 656 Phys., 21, 10589–10608, https://doi.org/10.5194/acp-21-10589-2021, 2021.
- 657 Claeys, M., Graham, B., Vas, G., Wang, W., Vermeylen, R., Pashynska, V., Cafmeyer, J., Guyon, P., Andreae,
- M. O., Artaxo, P., and Maenhaut, W.: Formation of Secondary Organic Aerosols Through Photooxidation
- of Isoprene, Science, 303, 1173–1176, https://doi.org/doi:10.1126/science.1092805, 2004.
- Claeys, M., Szmigielski, R., Kourtchev, I., Van der Veken, P., Vermeylen, R., Maenhaut, W., Jaoui, M.,
- Kleindienst, T. E., Lewandowski, M., Offenberg, J. H., and Edney, E. O.: Hydroxydicarboxylic Acids:
- Markers for Secondary Organic Aerosol from the Photooxidation of α-Pinene, Environ. Sci. Technol., 41,
- 663 1628–1634, https://doi.org/10.1021/es0620181, 2007.
- 664 Ding, X., Wang, X. M., Gao, B., Fu, X. X., He, Q. F., Zhao, X. Y., Yu, J. Z., and Zheng, M.: Tracer-based
- estimation of secondary organic carbon in the Pearl River Delta, south China, J. Geophys. Res-Atmos., 117,
- 666 https://doi.org/10.1029/2011JD016596, 2012.
- Ding, X., Wang, X. M., Xie, Z. Q., Zhang, Z., and Sun, L. G.: Impacts of Siberian Biomass Burning on
- Organic Aerosols over the North Pacific Ocean and the Arctic: Primary and Secondary Organic Tracers,
- Environ. Sci. Technol., 47, 3149–3157, https://doi.org/10.1021/es3037093, 2013.
- 670 Ding, X., He, Q. F., Shen, R. Q., Yu, Q. Q., and Wang, X. M.: Spatial distributions of secondary organic
- aerosols from isoprene, monoterpenes, β-caryophyllene, and aromatics over China during summer, J.
- 672 Geophys. Res-Atmos., 119, 11877–811891, https://doi.org/10.1002/2014JD021748, 2014.
- Duhl, T. R., Helmig, D., and Guenther, A.: Sesquiterpene emissions from vegetation: a review, Biogeosciences,
- 5, 761–777, https://doi.org/10.5194/bg-5-761-2008, 2008.
- Eddingsaas, N. C., Loza, C. L., Yee, L. D., Chan, M., Schilling, K. A., Chhabra, P. S., Seinfeld, J. H., and
- Wennberg, P. O.: α-pinene photooxidation under controlled chemical conditions-Part 2: SOA yield and
- 677 composition in low- and high-NO_x environments, Atmos. Chem. Phys., 12, 7413–7427,
- 678 https://doi.org/10.5194/acp-12-7413-2012, 2012.

- 679 Engling, G., He, J., Betha, R., and Balasubramanian, R.: Assessing the regional impact of indonesian biomass
- burning emissions based on organic molecular tracers and chemical mass balance modeling, Atmos. Chem.
- Phys., 14, 8043–8054, https://doi.org/10.5194/acp-14-8043-2014, 2014.
- Fabbri, D., Torri, C., Simoneit, B. R. T., Marynowski, L., Rushdi, A. I., and Fabiańska, M. J.: Levoglucosan
- and other cellulose and lignin markers in emissions from burning of Miocene lignites, Atmos. Environ., 43,
- 684 2286–2295, https://doi.org/10.1016/j.atmosenv.2009.01.030, 2009.
- 685 Fan, Y. B., Liu, C. Q., Li, L. J., Ren, L. J., Ren, H., Zhang, Z. M., Li, Q. K., Wang, S., Hu, W., Deng, J. J., Wu,
- 686 L. B., Zhong, S. J., Zhao, Y., Pavuluri, C. M., Li, X. D., Pan, X. L., Sun, Y. L., Wang, Z. F, Kawamura, K.,
- Shi, Z. B., and Fu, P. Q.: Large contributions of biogenic and anthropogenic sources to fine organic
- aerosols in Tianjin, North China, Atmos. Chem. Phys., 20, 117–137, https://doi.org/10.5194/acp-20-117-
- 689 2020, 2020.
- 690 Fry, J. L., Kiendler-Scharr, A., Rollins, A. W., Wooldridge, P. J., Brown, S. S., Fuchs, H., Dub é, W., Mensah,
- A., dal Maso, M., Tillmann, R., Dorn, H. P., Brauers, T., and Cohen, R. C.: Organic nitrate and secondary
- organic aerosol yield from NO₃ oxidation of β-pinene evaluated using a gas-phase kinetics/aerosol
- 693 partitioning model, Atmos. Chem. Phys., 9, 1431–1449, https://doi.org/10.5194/acp-9-1431-2009, 2009.
- 694 Fu, P. Q., Kawamura, K., Okuzawa, K., Aggarwal, S. G., Wang, G., Kanaya, Y., and Wang, Z.: Organic
- 695 molecular compositions and temporal variations of summertime mountain aerosols over Mt. Tai, North
- 696 China Plain, J. Geophys. Res-Atmos., 113, https://doi.org/10.1029/2008JD009900, 2008.
- 697 Fu, P. Q., Kawamura, K., and Barrie, L. A.: Photochemical and other sources of organic compounds in the
- 698 Canadian high arctic aerosol pollution during winter-spring, Environ. Sci. Technol., 43, 286–292,
- 699 https://doi.org/10.1021/es803046q, 2009.
- 700 Fu, P. Q., Kawamura, K., Pavuluri, C. M., Swaminathan, T., and Chen, J.: Molecular characterization of urban
- organic aerosol in tropical India: contributions of primary emissions and secondary photooxidation, Atmos.
- 702 Chem. Phys., 10, 2663–2689, https://doi.org/10, 2663-2689, 10.5194/acp-10-2663-2010, 2010.
- Fu, P. Q, Kawamura, K., and Miura, K.: Molecular characterization of marine organic aerosols collected
- during a round-the-world cruise, J. Geophys. Res-Atmos., 116, https://doi.org/10.1029/2011JD015604,
- 705 2011.
- 706 Fu, P. Q., Kawamura, K., Kobayashi, M., and Simoneit, B. R. T.: Seasonal variations of sugars in atmospheric
- 707 particulate matter from Gosan, Jeju Island: Significant contributions of airborne pollen and Asian dust in
- 708 spring, Atmos. Environ., 55, 234–239, https://doi.org/10.1016/j.atmosenv.2012.02.061, 2012.

- 709 Fu, P. Q., Kawamura, K., Chen, J., and Miyazaki, Y.: Secondary Production of Organic Aerosols from
- 710 Biogenic VOCs over Mt. Fuji, Japan, Environ. Sci. Technol., 48, 8491-8497,
- 711 https://doi.org/10.1021/es500794d, 2014.
- Graham, B., Guyon, P., Taylor, P. E., Artaxo, P., Maenhaut, W., Glovsky, M. M., Flagan, R. C., and Andreae,
- 713 M. O.: Organic compounds present in the natural Amazonian aerosol: Characterization by gas
- chromatography–mass spectrometry, J. Geophys. Res-Atmos., 108, https://doi.org/10.1029/2003JD003990,
- 715 2003.
- Guenther, A., Hewitt, C. N., Erickson, D., Fall, R., Geron, C., Graedel, T., Harley, P., Klinger, L., Lerdau, M.,
- Mckay, W. A., Pierce, T., Scholes, B., Steinbrecher, R., Tallamraju, R., Taylor, J., and Zimmerman, P.: A
- 718 global model of natural volatile organic compound emissions, Res-Atmos., 100, 8873–8892,
- 719 https://doi.org/10.1029/94JD02950, 1995.
- Guo, S., Hu, M., Guo, Q., Zhang, X., Zheng, M., Zheng, J., Chang, C. C., Schauer, J. J., and Zhang, R.:
- Primary Sources and Secondary Formation of Organic Aerosols in Beijing, China, Environ. Sci. Technol.,
- 722 46, 9846–9853, 10.1021/es2042564, 2012.
- Guo, W., Li, Z. C., Zhang, Z. Y., Zhu, R. G., Xiao, H. W., and Xiao, H. Y.: Sources and influences of
- atmospheric nonpolar organic compounds in Nanchang, central China: Full-year monitoring with a focus
- 725 on winter pollution episodes, Sci. Total Environ., 912, 169216,
- 726 https://doi.org/10.1016/j.scitotenv.2023.169216, 2024a.
- Guo, W., Zhang, Z. Y., Zhu, R. G., Li, Z. C., Liu, C., Xiao, H. W., and Xiao, H. Y.: Pollution characteristics,
- 728 sources, and health risks of phthalate esters in ambient air: A daily continuous monitoring study in the
- 729 central Chinese city of Nanchang, Chemosphere, 353, 141564,
- 730 https://doi.org/10.1016/j.chemosphere.2024.141564, 2024b.
- Hallquist, M., Wenger, J. C., Baltensperger, U., Rudich, Y., Simpson, D., Claeys, M., Dommen, J., Donahue,
- N. M., George, C., Goldstein, A. H., Hamilton, J. F., Herrmann, H., Hoffmann, T., Iinuma, Y., Jang, M.,
- Jenkin, M. E., Jimenez, J. L., Kiendler-Scharr, A., Maenhaut, W., McFiggans, G., Mentel, T. F., Monod, A.,
- Pr év ôt, A. S. H., Seinfeld, J. H., Surratt, J. D., Szmigielski, R., and Wildt, J.: The formation, properties and
- impact of secondary organic aerosol: current and emerging issues, Atmos. Chem. Phys., 9, 5155–5236,
- 736 10.5194/acp-9-5155-2009, 2009.
- Haque, M. M., Kawamura, K., Deshmukh, D. K., Fang, C., Song, W., Mengying, B., and Zhang, Y. L.:
- 738 Characterization of organic aerosols from a Chinese megacity during winter: predominance of fossil fuel
- 739 combustion, Atmos. Chem. Phys., 19, 5147–5164, 10.5194/acp-19-5147-2019, 2019.

- Haque, M. M., Zhang, Y., Bikkina, S., Lee, M., and Kawamura, K.: Regional heterogeneities in the emission
- of airborne primary sugar compounds and biogenic secondary organic aerosols in the East Asian outflow:
- evidence for coal combustion as a source of levoglucosan, Atmos. Chem. Phys., 22, 1373–1393,
- 743 10.5194/acp-22-1373-2022, 2022.
- Haque, M. M., Verma, S. K., Deshmukh, D. K., Kunwar, B., and Kawamura, K.: Seasonal characteristics of
- 5745 biogenic secondary organic aerosol tracers in a deciduous broadleaf forest in northern Japan, Chemosphere,
- 746 311, 136785, https://doi.org/10.1016/j.chemosphere.2022.136785, 2023.
- He, L. Y., Hu, M., Huang, X. F., Yu, B. D., Zhang, Y. H., and Liu, D. Q.: Measurement of emissions of fine
- particulate organic matter from Chinese cooking, Atmos. Environ., 38, 6557-6564,
- 749 https://doi.org/10.1016/j.atmosenv.2004.08.034, 2004.
- 750 He, L. Y., Hu, M., Huang, X. F., Zhang, Y. H., and Tang, X. Y.: Seasonal pollution characteristics of organic
- 751 compounds in atmospheric fine particles in Beijing, Sci. Total Environ., 359, 167–176,
- 752 https://doi.org/10.1016/j.scitotenv.2005.05.044, 2006.
- Helmig, D., Ortega, J., Guenther, A., Herrick, J. D., and Geron, C.: Sesquiterpene emissions from loblolly pine
- and their potential contribution to biogenic aerosol formation in the Southeastern US, Atmos. Environ., 40,
- 755 4150–4157, https://doi.org/10.1016/j.atmosenv.2006.02.035, 2006.
- Hoyle, C. R., Boy, M., Donahue, N. M., Fry, J. L., Glasius, M., Guenther, A., Hallar, A. G., Huff Hartz, K.,
- Petters, M. D., Pet ä ä, T., Rosenoern, T., and Sullivan, A. P.: A review of the anthropogenic influence on
- biogenic secondary organic aerosol, Atmos. Chem. Phys., 11, 321–343, https://doi.org/10.5194/acp-11-321-
- 759 2011, 2011.
- Huang, R. J., Zhang, Y., Bozzetti, C., Ho, K. F., Cao, J. J., Han, Y., Daellenbach, K. R., Slowik, J. G., Platt, S.
- M., Canonaco, F., Zotter, P., Wolf, R., Pieber, S. M., Bruns, E. A., Crippa, M., Ciarelli, G., Piazzalunga, A.,
- Schwikowski, M., Abbaszade, G., Schnelle-Kreis, J., Zimmermann, R., An, Z., Szidat, S., Baltensperger,
- 763 U., El Haddad, I., and Prevot, A. S.: High secondary aerosol contribution to particulate pollution during
- haze events in China, Nature, 514, 218–222, https://doi.org/10.1038/nature13774, 2014.
- Huebert, B., Bates, T., Russell, P., Shi, G., Kim, Y., Kawamura, K., Carmichael, G., and Nakajima, T.: An
- overview of ACE-Asia: Strategies for quantifying the relationships between Asian aerosols and their
- 767 climatic impacts, J. Geophys. Res-Atmos., https://doi.org/108, 10.1029/2003JD003550, 2003.
- Iinuma, Y., Brüggemann, E., Gnauk, T., Müller, K., Andreae, M. O., Helas, G., Parmar, R., and Herrmann, H.:
- Source characterization of biomass burning particles: The combustion of selected European conifers,
- 770 African hardwood, savanna grass, and German and Indonesian peat, J. Geophys. Res-Atmos., 112,
- 771 https://doi.org/10.1029/2006JD007120, 2007.

- 772 Iyer, S., Rissanen, M. P., Valiev, R., Barua, S., Krechmer, J. E., Thornton, J., Ehn, M., and Kurtén, T.:
- Molecular mechanism for rapid autoxidation in α-pinene ozonolysis, Nat. Commun., 12, 878,
- 774 10.1038/s41467-021-21172-w, 2021.
- Jaoui, M., Kleindienst, T. E., Lewandowski, M., Offenberg, J. H., and Edney, E. O.: Identification and
- Quantification of Aerosol Polar Oxygenated Compounds Bearing Carboxylic or Hydroxyl Groups. 2.
- Organic Tracer Compounds from Monoterpenes, Environ. Sci. Technol., 39, 5661-5673,
- 778 10.1021/es048111b, 2005.
- Jaoui, M., Szmigielski, R., Nestorowicz, K., Kolodziejczyk, A., Sarang, K., Rudzinski, K. J., Konopka, A.,
- Bulska, E., Lewandowski, M., and Kleindienst, T. E.: Organic Hydroxy Acids as Highly Oxygenated
- 781 Molecular (HOM) Tracers for Aged Isoprene Aerosol, Environ. Sci. Technol., 53, 14516–14527,
- 782 10.1021/acs.est.9b05075, 2019.
- Kanakidou, M., Seinfeld, J. H., Pandis, S. N., Barnes, I., Dentener, F. J., Facchini, M. C., Van Dingenen, R.,
- Ervens, B., Nenes, A., Nielsen, C. J., Swietlicki, E., Putaud, J. P., Balkanski, Y., Fuzzi, S., Horth, J.,
- Moortgat, G. K., Winterhalter, R., Myhre, C. E. L., Tsigaridis, K., Vignati, E., Stephanou, E. G., and
- Wilson, J.: Organic aerosol and global climate modelling: a review, Atmos. Chem. Phys., 5, 1053–1123,
- 787 https://doi.org/10.5194/acp-5-1053-2005, 2005.
- 788 Kawamura, K., and Gagosian, R. B.: Implications of ω-oxocarboxylic acids in the remote marine atmosphere
- for photo-oxidation of unsaturated fatty acids, Nature, 325, 330–332, https://doi.org/10.1038/325330a0,
- 790 1987.
- 791 Kawamura, K., and Kaplan, I. R.: Motor exhaust emissions as a primary source for dicarboxylic acids in Los
- Angeles ambient air, Environ. Sci. Technol., 21, 105–110, https://doi.org/10.1021/es00155a014, 1987.
- 793 Kawamura, K., and Ikushima, K.: Seasonal changes in the distribution of dicarboxylic acids in the urban
- 794 atmosphere, Environ. Sci. Technol., 27, 2227–2235, https://doi.org/10.1021/ES00047A033, 1993.
- 795 Kawamura, K., and Sakaguchi, F.: Molecular distributions of water soluble dicarboxylic acids in marine
- aerosols over the Pacific Ocean including tropics, J. Geophys. Res-Atmos., 104, 3501-3509,
- 797 https://doi.org/10.1029/1998JD100041, 1999.
- 798 Kawamura, K., Steinberg, S., and Kaplan, I. R.: Homologous series of C1–C10 monocarboxylic acids and C1–
- 799 C6 carbonyls in Los Angeles air and motor vehicle exhausts, Atmos. Environ., 34, 4175–4191,
- 800 https://doi.org/10.1016/S1352-2310(00)00212-0, 2000.
- 801 Kawamura, K., Ishimura, Y., and Yamazaki, K.: Four years' observations of terrestrial lipid class compounds
- in marine aerosols from the western North Pacific, Global Biogeochem. Cy., 17, 1003,
- 803 https://doi.org/10.1029/2001GB001810, 2003.

- Kleindienst, T. E., Jaoui, M., Lewandowski, M., Offenberg, J. H., Lewis, C. W., Bhave, P. V., and Edney, E.
- O.: Estimates of the contributions of biogenic and anthropogenic hydrocarbons to secondary organic
- 806 aerosol at a southeastern US location, Atmos. Environ., 41, 8288-8300,
- 807 https://doi.org/10.1016/j.atmosenv.2007.06.045, 2007.
- 808 Kleindienst, T. E., Lewandowski, M., Offenberg, J. H., Jaoui, M., and Edney, E. O.: The formation of
- secondary organic aerosol from the isoprene ⁺OH reaction in the absence of NO_x, Atmos. Chem. Phys., 9,
- 810 6541–6558, 10.5194/acp-9-6541-2009, 2009.
- 811 Kleindienst, T.E., Jaoui, M., Lewandowski, M., Offenberg, J.H., and Docherty, K.S.: The formation of SOA
- and chemical tracer compounds from the photooxidation of naphthalene and its methyl analogs in the
- presence and absence of nitrogen oxides, Atmos. Chem. Phys., 12, 8711–8726 https://doi.org/10.5194/acp-
- 814 12-8711-2012, 2012.
- 815 Kunwar, B., and Kawamura, K.: One-year observations of carbonaceous and nitrogenous components and
- major ions in the aerosols from subtropical Okinawa Island, an outflow region of Asian dusts, Atmos.
- 817 Chem. Phys., 14, 1819–1836, https://doi.org/10.5194/acp-14-1819-2014, 2014.
- Lewandowski, M., Jaoui, M., Offenberg, J. H., Kleindienst, T. E., Edney, E. O., Sheesley, R. J., and Schauer, J.
- J.: Primary and secondary contributions to ambient PM in the midwestern United States, Environ. Sci.
- Technol., 42, 3303–3309, https://doi.org/doi: 10.1021/es0720412, 2008.
- Lewandowski, M., Piletic, I. R., Kleindienst, T. E., Offenberg, J. H., Beaver, M. R., Jaoui, M., Docherty, K. S.,
- and Edney, E. O.: Secondary organic aerosol characterisation at field sites across the United States during
- the spring-summer period, Int. J. Environ. An. Ch., 93, 1084–1103,
- 824 https://doi.org/10.1080/03067319.2013.803545, 2013.
- 825 Li, J. J., Wang, G. H., Wu, C., Cao, C., Ren, Y.Q., Wang, J. Y., Li, J., Cao, J. J., Zeng, L. M., and Zhu, T.:
- Characterization of isoprene-derived secondary organic aerosols at a rural site in North China Plain with
- implications for anthropogenic pollution effects, Sci. Rep-Uk., 8, 535, https://doi.org/10.1038/s41598-017-
- 828 18983-7, 2018.
- 829 Li, J. J., Wang, G. H., Zhang, Q., Li, J., Wu, C., Jiang, W. Q., Zhu, T., and Zeng, L. M.: Molecular
- 830 characteristics and diurnal variations of organic aerosols at a rural site in the North China Plain with
- implications for the influence of regional biomass burning, Atmos. Chem. Phys., 19, 10481–
- https://doi.org/10496, 10.5194/acp-19-10481-2019, 2019.
- 833 Lin, Y. H., Zhang, Z., Docherty, K. S., Zhang, H., Budisulistiorini, S. H., Rubitschun, C. L., Shaw, S. L.,
- Knipping, E. M., Edgerton, E. S., Kleindienst, T. E., Gold, A., and Surratt, J. D.: Isoprene Epoxydiols as

- Precursors to Secondary Organic Aerosol Formation: Acid-Catalyzed Reactive Uptake Studies with
- 836 Authentic Compounds, Environ. Sci. Technol., 46, 250–258, https://doi.org/10.1021/es202554c, 2012.
- Lin, Y. H., Knipping, E. M., Edgerton, E. S., Shaw, S. L., and Surratt, J. D.: Investigating the influences of
- SO₂ and NH₃ levels on isoprene-derived secondary organic aerosol formation using conditional sampling
- 839 approaches, Atmos. Chem. Phys., 13, 8457–8470, https://doi.org/10.5194/acp-13-8457-2013, 2013.
- Liu, D., Xu, S. F., Lang, Y. C., Hou, S. J., Wei, L. F., Pan, X. L., Sun, Y. L., Wang, Z. F., Kawamura, K., and
- Fu, P. Q.: Size distributions of molecular markers for biogenic secondary organic aerosol in urban Beijing,
- 842 Environ. Pollut., 327, 121569, https://doi.org/10.1016/j.envpol.2023.121569, 2023.
- Ng, N. L., Brown, S. S., Archibald, A. T., Atlas, E., Cohen, R. C., Crowley, J. N., Day, D. A., Donahue, N. M.,
- Fry, J. L., Fuchs, H., Griffin, R. J., Guzman, M. I., Herrmann, H., Hodzic, A., Iinuma, Y., Jimenez, J. L.,
- Kiendler-Scharr, A., Lee, B. H., Luecken, D. J., Mao, J., McLaren, R., Mutzel, A., Osthoff, H. D., Ouyang,
- B., Picquet-Varrault, B., Platt, U., Pye, H. O. T., Rudich, Y., Schwantes, R. H., Shiraiwa, M., Stutz, J.,
- Thornton, J. A., Tilgner, A., Williams, B. J., and Zaveri, R. A.: Nitrate radicals and biogenic volatile
- organic compounds: oxidation, mechanisms, and organic aerosol, Atmos. Chem. Phys., 17, 2103–2162,
- https://doi.org/10.5194/acp-17-2103-2017, 2017.
- Nguyen, T. B., Bates, K. H., Crounse, J. D., Schwantes, R. H., Zhang, X., Kjaergaard, H. G., Surratt, J. D., Lin,
- 851 P., Laskin, A., Seinfeld, J. H., and Wennberg, P. O.: Mechanism of the hydroxyl radical oxidation of
- 852 methacryloyl peroxynitrate (MPAN) and its pathway toward secondary organic aerosol formation in the
- atmosphere, Chem. Phys., 17, 17914–17926, https://doi.org/10.1039/c5cp02001h, 2015.
- Nolte, C. G., Schauer, J. J., Cass, G. R., and Simoneit, B. R. T.: Highly Polar Organic Compounds Present in
- Meat Smoke, Environ. Sci. Technol., 33, 3313–3316, https://doi.org/10.1021/es990122v, 1999.
- Nolte, C. G., Schauer, J. J., Cass, G. R., and Simoneit, B. R. T.: Highly Polar Organic Compounds Present in
- Wood Smoke and in the Ambient Atmosphere, Environ. Sci. Technol., 35, 1912–1919,
- https://doi.org/10.1021/es001420r, 2001.
- Nozi ère, B., Gonz ález, N. J. D., Borg-Karlson, A. K., Pei, Y. X., Redeby, J. P., Krejci, R., Dommen, J., Pr év ât,
- A. S. H., and Anthonsen, T.: Atmospheric chemistry in stereo: A new look at secondary organic aerosols
- from isoprene, Geophys. Res. Lett., 38, https://doi.org/10.1029/2011GL047323, 2011.
- 862 Oros, D. R., and Simoneit, B. R. T.: Identification and emission rates of molecular tracers in coal smoke
- 863 particulate matter, Fuel, 79, 515–536, https://doi.org/10.1016/S0016-2361(99)00153-2, 2000.
- Oros, D. R., and Simoneit, B. R. T.: Identification and emission factors of molecular tracers in organic aerosols
- from biomass burning Part 2. Deciduous trees, Appl. Geochem., 16, 1545–1565,
- https://doi.org/10.1016/S0883-2927(01)00022-1, 2001.

- Piccot, S. D., Watson, J. J., and Jones, J. W.: A global inventory of volatile organic compound emissions from
- anthropogenic sources, J. Geophys. Res., 97, 9897–9912, https://doi.org/10.1029/92JD00682, 1992.
- 869 Puxbaum, H., and Tenze-Kunit, M.: Size distribution and seasonal variation of atmospheric cellulose, Atmos.
- 870 Environ., 37, 3693–3699, https://doi.org/10.1016/S1352-2310(03)00451-5, 2003.
- 871 Ren, H., Hu, W., Wei, L. F., Yue, S. Y., Zhao, J., Li, L. J., Wu, L. B., Zhao, W. Y., Ren, L. J., Kang, M. J., Xie,
- Q. Y., Su, S. H., Pan, X. L., Wang, Z. F., Sun, Y. L., Kawamura, K., and Fu, P. Q.: Measurement report:
- Vertical distribution of biogenic and anthropogenic secondary organic aerosols in the urban boundary layer
- 874 over Beijing during late summer, Atmos. Chem. Phys., 21, 12949–12963, https://doi.org/10.5194/acp-21-
- 875 12949-2021, 2021.
- 876 Ren, Y. Q., Wang, G. H., Tao, J., Zhang, Z. S., Wu, C., Wang, J. Y., Li, J. J., Wei, J., Li, H., and Meng, F.:
- 877 Seasonal characteristics of biogenic secondary organic aerosols at Mt. Wuyi in Southeastern China:
- 878 Influence of anthropogenic pollutants, Environ. Pollut., 252, 493–500,
- https://doi.org/10.1016/j.envpol.2019.05.077, 2019.
- Riipinen, I., Yli-Juuti, T., Pierce, J. R., Petaja, T., Worsnop, D. R., Kulmala, M., and Donahue, N. M.: The
- contribution of organics to atmospheric nanoparticle growth, Nat. Geosci., 5, 453-458,
- https://doi.org/10.1038/ngeo1499, 2012.
- 883 Rogge, W. F., Hildemann, L. M., Mazurek, M. A., Cass, G. R., and Simoneit, B. R. T.: Sources of fine organic
- aerosol. 1. Charbroilers and meat cooking operations, Environ. Sci. Technol., 25, 1112–1125,
- https://doi.org/10.1021/es00018a015, 1991.
- 886 Rogge, W. F., Hildemann, L. M., Mazurek, M. A., Cass, G. R., Simoneit, B. R. T. J. E. S., and Technology:
- Sources of fine organic aerosol. 2. Noncatalyst and catalyst-equipped automobiles and heavy-duty diesel
- trucks, Environ. Sci. Technol., 27, 636–651, https://doi.org/10.1021/es00041a007, 1993.
- 889 Rogge, W. F., Medeiros, P. M., and Simoneit, B. R. T.: Organic marker compounds for surface soil and
- 890 fugitive dust from open lot dairies and cattle feedlots, Atmos. Environ., 40, 27–49,
- 891 https://doi.org/10.1016/j.atmosenv.2005.07.076, 2006.
- 892 Rudich, Y., Donahue, N. M., and Mentel, T. F.: Aging of organic aerosol: bridging the gap between laboratory
- 893 and field studies, Annu. Rev. Phys. Chem., 58, 321–352,
- https://doi.org/10.1146/annurev.physchem.58.032806.104432, 2007.
- 895 Rybicki, M., Marynowski, L., Bechtel, A., and Simoneit, B. R. T.: Variations in δ13C values of levoglucosan
- from low-temperature burning of lignite and biomass, Sci. Total Environ., 733, 138991,
- 897 https://doi.org/10.1016/j.scitotenv.2020.138991, 2020a.

- 898 Rybicki, M., Marynowski, L., and Simoneit, B. R. T.: Composition of organic compounds from low-
- temperature burning of lignite and their application as tracers in ambient air, Chemosphere, 249, 126087,
- 900 https://doi.org/10.1016/j.chemosphere.2020.126087, 2020b.
- 901 Saarikoski, S., Timonen, H., Saarnio, K., Aurela, M., Järvi, L., Keronen, P., Kerminen, V. M., and Hillamo, R.:
- Sources of organic carbon in fine particulate matter in northern European urban air, Atmos. Chem. Phys., 8,
- 903 6281–6295, https://doi.org/10.5194/acp-8-6281-2008, 2008.
- 904 Sharkey, T. D., Wiberley, A. E., and Donohue, A. R.: Isoprene emission from plants: why and how, Annals of
- 905 botany, 101, 5–18, https://doi.org/10.1093/aob/mcm240, 2008.
- Sheesley, R. J., Schauer, J. J., Chowdhury, Z., Cass, G. R., and Simoneit, B. R. T.: Characterization of organic
- 907 aerosols emitted from the combustion of biomass indigenous to South Asia, J. Geophys. Res-Atmos., 108,
- 908 https://doi.org/10.1029/2002JD002981, 2003.
- 909 Shiraiwa, M., Ueda, K., Pozzer, A., Lammel, G., Kampf, C. J., Fushimi, A., Enami, S., Arangio, A. M.,
- 910 Fröhlich-Nowoisky, J., Fujitani, Y., Furuyama, A., Lakey, P. S. J., Lelieveld, J., Lucas, K., Morino, Y.,
- Pöschl, U., Takahama, S., Takami, A., Tong, H., Weber, B., Yoshino, A., and Sato, K.: Aerosol Health
- 912 Effects from Molecular to Global Scales, Environ. Sci. Technol., 51, 13545-13567,
- 913 10.1021/acs.est.7b04417, 2017.
- 914 Simoneit, B. R. T.: Biomass burning a review of organic tracers for smoke from incomplete combustion,
- 915 Applied Geochemistry, 17, 129–162, https://doi.org/10.1016/S0883-2927(01)00061-0, 2002.
- 916 Simoneit, B. R. T., Kobayashi, M., Mochida, M., Kawamura, K., and Huebert, B. J.: Aerosol particles
- 917 collected on aircraft flights over the northwestern Pacific region during the ACE-Asia campaign:
- Composition and major sources of the organic compounds, J. Geophys. Res-Atmos., 109,
- 919 https://doi.org/10.1029/2004JD004565, 2004a.
- 920 Simoneit, B. R., Elias, V. O., Kobayashi, M., Kawamura, K., Rushdi, A. I., Medeiros, P. M., Rogge, W. F.,
- 921 and Didyk, B. M.: Sugars-dominant water-soluble organic compounds in soils and characterization as
- 922 tracers in atmospheric particulate matter, Environ. Sci. Technol., 38, 5939-5949,
- 923 https://doi.org/10.1021/es0403099, 2004b.
- 924 Srivastava, D., Vu, T. V., Tong, S., Shi, Z., and Harrison, R. M.: Formation of secondary organic aerosols
- 925 from anthropogenic precursors in laboratory studies, Npj. Clim. Atmos. Sci., 5, 22,
- 926 https://doi.org/10.1038/s41612-022-00238-6, 2022.
- 927 Stohl, A., Berg, T., Burkhart, J. F., Fjéraa, A. M., Forster, C., Herber, A., Hov, Ø., Lunder, C., McMillan, W.
- 928 W., Oltmans, S., Shiobara, M., Simpson, D., Solberg, S., Stebel, K., Ström, J., Tørseth, K., Treffeisen, R.,
- Virkkunen, K., and Yttri, K. E.: Arctic smoke record high air pollution levels in the European

- Arctic due to agricultural fires in Eastern Europe in spring 2006, Atmos. Chem. Phys., 7, 511-534,
- 931 https://doi.org/10.5194/acp-7-511-2007, 2007.
- 932 Stone, E. A., Zhou, J., Snyder, D. C., Rutter, A. P., Mieritz, M., and Schauer, J. J.: A comparison of
- 933 summertime secondary organic aerosol source contributions at contrasting urban locations, Environ. Sci.
- 934 Technol., 43, 3448–3454, https://doi.org/10.1021/es8025209, 2009.
- 935 Surratt, J. D., Murphy, S. M., Kroll, J. H., Ng, N. L., Hildebrandt, L., Sorooshian, A., Szmigielski, R.,
- 936 Vermeylen, R., Maenhaut, W., Claeys, M., Flagan, R. C., and Seinfeld, J. H.: Chemical Composition of
- 937 Secondary Organic Aerosol Formed from the Photooxidation of Isoprene, J. Phys. Chem. A, 110, 9665–
- 938 9690, 10.1021/jp061734m, 2006.
- 939 Surratt, J. D., Chan, A. W. H., Eddingsaas, N. C., Chan, M., Loza, C. L., Kwan, A. J., Hersey, S. P., Flagan, R.
- 940 C., Wennberg, P. O., and Seinfeld, J. H.: Reactive intermediates revealed in secondary organic aerosol
- 941 formation from isoprene, Proc. Natl. Acad. Sci. U.S.A., 107, 6640-6645,
- 942 https://doi.org/doi:10.1073/pnas.0911114107, 2010.
- Tang, T. G., Cheng, Z. N., Xu, B. Q., Zhang, B. L., Li, J., Zhang, W., Wang, K. L., and Zhang, G.: Source
- Diversity of Intermediate Volatility n-Alkanes Revealed by Compound-Specific δ^{13} C- δ D Isotopes, Environ.
- 945 Sci. Technol., 56, 14262–14271, 10.1021/acs.est.2c02156, 2022.
- 946 Turpin, B. J., and Huntzicker, J. J.: Identification of secondary organic aerosol episodes and quantitation of
- primary and secondary organic aerosol concentrations during SCAQS, Atmos. Environ., 29, 3527–3544,
- 948 https://doi.org/10.1016/1352-2310(94)00276-Q, 1995.
- von Schneidemesser, E., Zhou, J., Stone, E. A., Schauer, J. J., Shpund, J., Brenner, S., Qasrawi, R., Abdeen, Z.,
- and Sarnat, J. A.: Spatial Variability of Carbonaceous Aerosol Concentrations in East and West Jerusalem,
- 951 Environ. Sci. Technol., 44, 1911–1917, https://doi.org/10.1021/es9014025, 2010.
- Wang, G. H., and Kawamura, K.: Molecular Characteristics of Urban Organic Aerosols from Nanjing: A Case
- 953 Study of A Mega-City in China, Environ. Sci. Technol., 39, 7430–7438, https://doi.org/10.1021/es051055,
- 954 2005.
- 955 Wang, G. H., Kawamura, K., Lee, S., Ho, K., and Cao, J. J.: Molecular, Seasonal, and Spatial Distributions of
- 956 Organic Aerosols from Fourteen Chinese Cities, Environ. Sci. Technol., 40, 4619-4625,
- 957 https://doi.org/10.1021/es060291x, 2006.
- 958 Wang, G. H., Kawamura, K., Hatakeyama, S., Takami, A., Li, H., and Wang, W.: Aircraft Measurement of
- Organic Aerosols over China, Environ. Sci. Technol., 41, 3115–3120, https://doi.org/10.1021/es062601h,
- 960 2007.

- 961 Wang, Y., Pavuluri, C. M., Fu, P. Q., Li, P. S., Dong, Z. C., Xu, Z. J., Ren, H., Fan, Y. B., Li, L. J., Zhang, Y.
- L., and Liu, C. Q.: Characterization of Secondary Organic Aerosol Tracers over Tianjin, North China
- during Summer to Autumn, Acs Earth Space Chem., 3, 2339–2352, 10.1021/acsearthspacechem.9b00170,
- 964 2019.
- Weber, R. J., Sullivan, A. P., Peltier, R. E., Russell, A. G., Yan, B., Zheng, M., Gouw, J. d., Warneke, C.,
- 966 Brock, C. A., Holloway, J. S., Atlas, E. L., and Edgerton, E. S.: A study of secondary organic aerosol
- formation in the anthropogenic-influenced southeastern United States, J. Geophys. Res-Atmos., 112,
- 968 https://doi.org/10.1029/2007JD008408, 2007.
- 969 Wu, J. R., Bei, N. F., Wang, Y., Li, X., Liu, S. X., Liu, L., Wang, R. N., Yu, J. Y., Le, T. H., Zuo, M., Shen, Z.
- 970 X., Cao, J. J., Tie, X. X., and Li, G. H.: Insights into particulate matter pollution in the North China Plain
- during wintertime: local contribution or regional transport?, Atmos. Chem. Phys., 21, 2229–2249,
- 972 https://doi.org/10.5194/acp-21-2229-2021, 2021.
- 973 Xu, B. Q., Tang, J., Tang, T. G., Zhao, S. Z., Zhong, G. C., Zhu, S. Y., Li, J., and Zhang, G.: Fates of
- 974 secondary organic aerosols in the atmosphere identified from compound-specific dual-carbon isotope
- 975 analysis of oxalic acid, Atmos. Chem. Phys., 23, 1565–1578, https://doi.org/10.5194/acp-23-1565-2023,
- 976 2023.
- Yu, B. Q., Zhang, G., Gustafsson, Ö., Kawamura, K., Li, J., Andersson, A., Bikkina, S., Kunwar, B., Pokhrel,
- 978 A., Zhong, G. C., Zhao, S. Z., Li, J., Huang, C., Cheng, Z. N., Zhu, S. Y., Peng, P. A., and Sheng, G. Y.:
- 279 Large contribution of fossil-derived components to aqueous secondary organic aerosols in China, Nat.
- 980 Commun., 13, 5115, https://doi.org/10.1038/s41467-022-32863-3, 2022.
- 981 Xu, J. S., Liu, D., Wu, X. F., Vu, T. V., Zhang, Y. L., Fu, P. Q., Sun, Y. L., Xu, W. Q., Zheng, B., Harrison, R.
- 982 M., and Shi, Z. B.: Source apportionment of fine organic carbon at an urban site of Beijing using a
- 983 chemical mass balance model, Atmos. Chem. Phys., 21, 7321–7341, https://doi.org/10.5194/acp-21-7321-
- 984 2021, 2021.
- 985 Yan, C. C., Sullivan, A. P., Cheng, Y., Zheng, M., Zhang, Y. H., Zhu, T., and Collett, J. L.: Characterization of
- 986 saccharides and associated usage in determining biogenic and biomass burning aerosols in atmospheric fine
- particulate matter in the North China Plain, Sci. Total Environ., 650, 2939–2950,
- 988 https://doi.org/10.1016/j.scitotenv.2018.09.325, 2019.
- 989 Yang, C., Hong, Z. Y., Chen, J. S., Xu, L. L., Zhuang, M. Z., and Huang, Z.: Characteristics of secondary
- organic aerosols tracers in PM2.5 in three central cities of the Yangtze river delta, China, Chemosphere,
- 991 293, 133637, https://doi.org/10.1016/j.chemosphere.2022.133637, 2022.

- 992 Yazdani, A., Dudani, N., Takahama, S., Bertrand, A., Pr év ât, A. S. H., El Haddad, I., and Dillner, A. M.:
- 993 Characterization of primary and aged wood burning and coal combustion organic aerosols in an
- environmental chamber and its implications for atmospheric aerosols, Atmos. Chem. Phys., 21, 10273–
- 995 10293, https://doi.org/10.5194/acp-21-10273-2021, 2021.
- Yee, L. D., Isaacman-VanWertz, G., Wernis, R. A., Kreisberg, N. M., Glasius, M., Riva, M., Surratt, J. D., de
- 997 Sá S. S., Martin, S. T., Alexander, M. L., Palm, B. B., Hu, W., Campuzano-Jost, P., Day, D. A., Jimenez, J.
- 998 L., Liu, Y., Misztal, P. K., Artaxo, P., Viegas, J., Manzi, A., de Souza, R. A. F., Edgerton, E. S., Baumann,
- 999 K., and Goldstein, A. H.: Natural and Anthropogenically Influenced Isoprene Oxidation in Southeastern
- 1000 United States and Central Amazon, Environ. Sci. Technol., 54, 5980-5991,
- 1001 https://doi.org/10.1021/acs.est.0c00805, 2020.
- 1002 Yttri, K. E., Dye, C., and Kiss, G.: Ambient aerosol concentrations of sugars and sugar-alcohols at four
- different sites in Norway, Atmos. Chem. Phys., 7, 4267–4279, https://doi.org/10.5194/acp-7-4267-2007,
- 1004 2007.
- 1005 Yuan, Q., Lai, S. C., Song, J. W., Ding, X., Zheng, L. S., Wang, X. M., Zhao, Y., Zheng, J. Y., Yue, D. L.,
- Zhong, L. J., Niu, X. J., and Zhang, Y. Y.: Seasonal cycles of secondary organic aerosol tracers in rural
- Guangzhou, Southern China: The importance of atmospheric oxidants, Environ. Pollut., 240, 884–893,
- 1008 https://doi.org/10.1016/j.envpol.2018.05.009, 2018.
- 1009 Zhang, Q., He, K. B., and Huo, H.: Cleaning China's air, Nature, 484, 161-162,
- 1010 https://doi.org/10.1038/484161a, 2012.
- 1011 Zhang, Q., Hu, W., Ren, H., Yang, J. B., Deng, J. J., Wang, D. W., Sun, Y. L., Wang, Z. F., Kawamura, K.,
- and Fu, P. Q.: Diurnal variations in primary and secondary organic aerosols in an eastern China coastal city:
- The impact of land-sea breezes, Environ. Pollut., 319, 121016,
- 1014 https://doi.org/10.1016/j.envpol.2023.121016, 2023.
- Zhang, X., McVay, R. C., Huang, D. D., Dalleska, N. F., Aumont, B., Flagan, R. C., and Seinfeld, J. H.:
- 1016 Formation and evolution of molecular products in α-pinene secondary organic aerosol, Proc. Natl. Acad.
- 1017 Sci. U. S. A., 112, 14168–14173, https://doi.org/10.1073/pnas.1517742112, 2015.
- 1018 Zhang, Y. X., Cao, F., Song, W. H., Jia, X. F., Xie, T., Wu, C.L., Yan, P., Yu, M. Y., Rauber, M., Salazar, G.,
- 1019 Szidat, S., and Zhang, Y. L.: Fossil and Nonfossil Sources of Winter Organic Aerosols in the Regional
- Background Atmosphere of China, Environ. Sci. Technol., 58, 1244–1254,
- 1021 https://doi.org/10.1021/acs.est.3c08491, 2024.

- 1022 Zhang, Y. X., Schauer, J. J., Zhang, Y. H., Zeng, L. M., Wei, Y. J., Liu, Y., and Shao, M.: Characteristics of
- Particulate Carbon Emissions from Real-World Chinese Coal Combustion, Environ. Sci. Technol., 42,
- 1024 5068–5073, https://doi.org/10.1021/es7022576, 2008.
- Zhang, Y. L., Kawamura, K., Agrios, K., Lee, M., Salazar, G., and Szidat, S.: Fossil and Nonfossil Sources of
- Organic and Elemental Carbon Aerosols in the Outflow from Northeast China, Environ. Sci. Technol., 50,
- 1027 6284–6292, https://doi.org/10.1021/acs.est.6b00351, 2016.
- 1028 Zhang, Y. X., Shao, M., Zhang, Y.H., Zeng, L.M., He, L.Y., Zhu, B., Wei, Y.J., and Zhu, X.L.: Source profiles
- of particulate organic matters emitted from cereal straw burnings, J. Environ. Sci., 19, 167-175,
- 1030 https://doi.org/10.1016/S1001-0742(07)60027-8, 2007.
- 1031 Zheng, M., Cass, G. R., Schauer, J. J., and Edgerton, E. S.: Source apportionment of PM2.5 in the
- Southeastern United States using solvent-extractable organic compounds as tracers, Environ. Sci. Technol.,
- 36, 2361–2371, https://doi.org/10.1021/es011275x, 2002.
- 2034 Zhao, Y. L., Hu, M., Slanina, S., and Zhang, Y. H.: Chemical Compositions of Fine Particulate Organic Matter
- Emitted from Chinese Cooking, Environ. Sci. Technol., 41, 99–105, https://doi.org/10.1021/es0614518,
- 1036 2007.
- 2037 Zhu, C. M., Kawamura, K., and Fu, P. Q.: Seasonal variations of biogenic secondary organic aerosol tracers in
- 1038 Cape Hedo, Okinawa, Atmos. Environ., 130, 113–119, https://doi.org/10.1016/j.atmosenv.2015.08.069,
- 1039 2016.
- Zhu, R. G., Xiao, H. Y., Cheng, L., Zhu, H., Xiao, H., and Gong, Y. Y.: Measurement report: Characterization
- of sugars and amino acids in atmospheric fine particulates and their relationship to local primary sources,
- 1042 Atmos. Chem. Phys., 22, 14019–14036, 10.5194/acp-22-14019-2022, 2022.

1045

1046

1047

1048

1050 **Figure Captions** 1051 Figure 1. One-year time series of organic carbon (OC), elemental carbon (EC), OC/EC ratios, PM_{2.5} levels, and 1052 concentrations of polar organic compounds. 1053 Figure 2. Molecular characteristics and seasonal variations of the major polar compounds in PM_{2.5}. The bars in 1054 the figure show the average concentrations of different compounds for each season, while the caps on the bars 1055 represent the standard deviations of these averages. The letters a, b, c, and d above the caps indicate whether 1056 the average concentrations differ significantly between seasons. Data points that do not share the same letter 1057 are significantly different, whereas those with the same letter are not significantly different, at the 95% 1058 confidence level. The Tukey test was used to assess the statistical significance of these differences. It should be 1059 noted that the same method was used to compare the statistical significance of differences between the data in 1060 the other figures presented later in the article. 1061 Figure 3. Molecular characteristics and seasonal variations of the minor polar compounds in $PM_{2.5}$. The 1062 explanations for the letters a, b, c, and d on the bars are provided in the caption of Figure 2. Figure 4. Molecular characteristics and seasonal variations of the SOA tracers in PM_{2.5}. The explanations for 1063 1064 the letters a, b, c, and d on the bars are provided in the caption of Figure 2. 1065 Figure 5. Concentrations and relative abundances of primary organic carbon (POC) from biomass burning 1066 (POC_{bb}), coal combustion (POC_{cc}), vehicle exhaust (POC_{ve}), cooking (POC_c), plant debris (POC_{pd}), and fungal 1067 spores (POC_{1s}), as well as secondary organic carbon (SOC) from isoprene (SOC₁), α/β -pinene (SOC_p), β -1068 caryophyllene (SOC_t), toluene (SOC_t), and naphthalene (SOC_n). POC and SOC concentrations were estimated 1069 using a tracer-based method, while other organic carbon (OOC) was calculated by subtracting the estimated 1070 OC from the measured OC. Winter-P refers to winter pollution periods, and Winter-R denotes the winter 1071 remainder. 1072 Figure 6. Pearson correlations between POC, SOC, and the measured OC for the annual sampling period (a), 1073 winter pollution periods (b), winter remainder (c), and individual pollution episodes in winter (d-l). The size of 1074 each circle represents the contribution (%) of POC and SOC to the variation in measured OC, as determined by 1075 redundancy analysis. Magenta circles indicate P-values from correlation and redundancy analyses less than 1076 0.05, while gray circles denote P-values greater than 0.05. Definitions: POC_{bb} (biomass burning), POC_{cc} (coal

combustion), POCve (vehicle exhaust), POCc (cooking), POCpd (plant debris), POCfs (fungal spores), and POC_{EC-based} (based on the EC method). SOC_i, SOC_p, SOC_c, SOC_t, SOC_n, and SOC_{EC-based} correspond to SOC from isoprene, α/β -pinene, β -caryophyllene, toluene, naphthalene, and EC-based methods, respectively. Figure 7. Linear correlations between temperature, NO₂, and SOC for the annual sampling periods (a), winter pollution periods (b), winter remainder (c), and individual winter pollution episodes (d–l). SOC concentrations were estimated using a tracer-based method. Winter-P refers to the winter pollution periods, while Winter-R denotes the winter remainder. PE1-PE9 correspond to winter pollution episodes 1-9.



Figure 1. One-year time series of organic carbon (OC), elemental carbon (EC), OC/EC ratios, $PM_{2.5}$ levels, and concentrations of polar organic compounds.

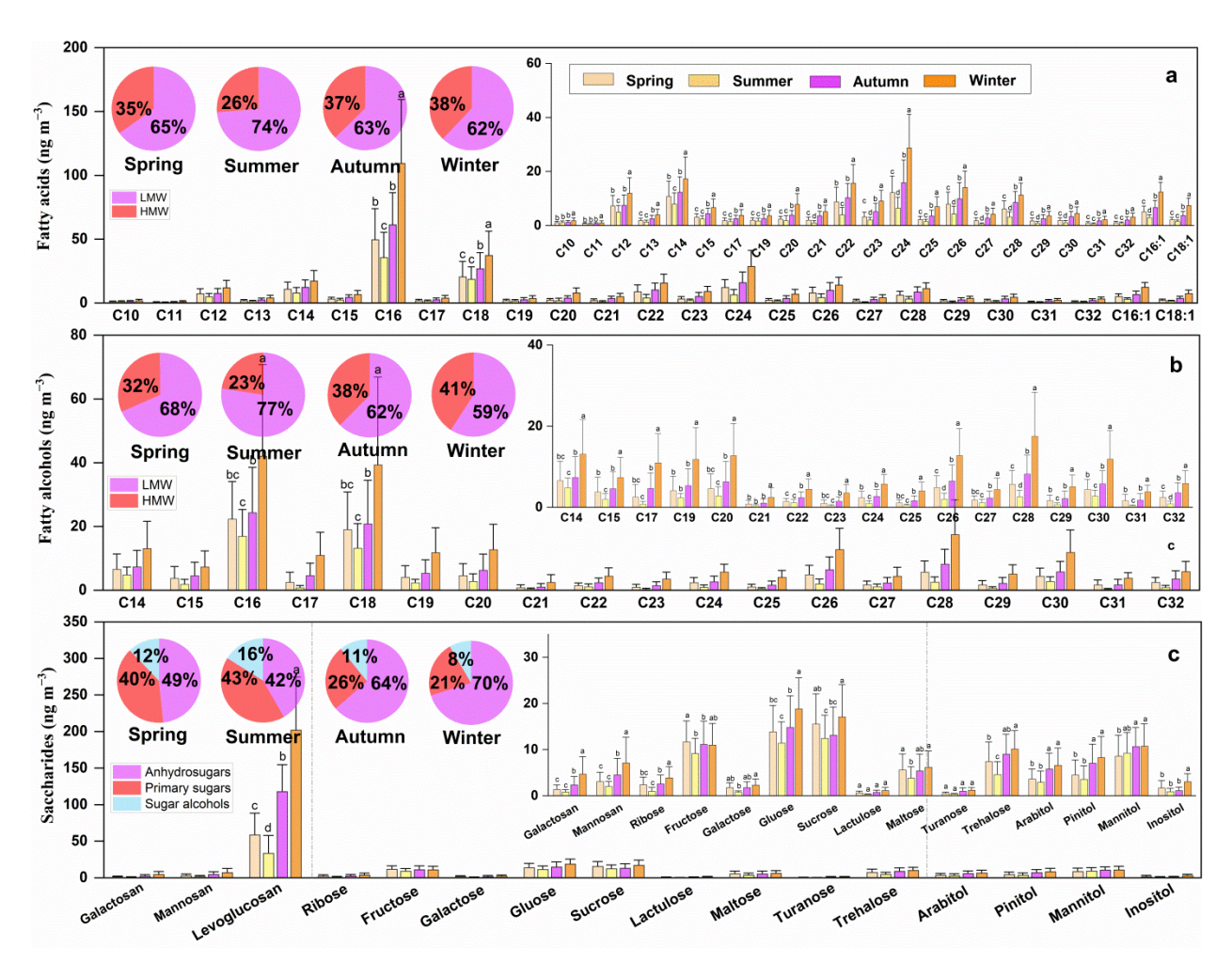


Figure 2. Molecular characteristics and seasonal variations of the major polar compounds in PM_{2.5}. The bars in the figure show the average concentrations of different compounds for each season, while the caps on the bars represent the standard deviations of these averages. The letters a, b, c, and d above the caps indicate whether the average concentrations differ significantly between seasons. Data points that do not share the same letter are significantly different, whereas those with the same letter are not significantly different, at the 95% confidence level. The Tukey test was used to assess the statistical significance of these differences. It should be noted that the same method was used to compare the statistical significance of differences between the data in the other figures presented later in the article.

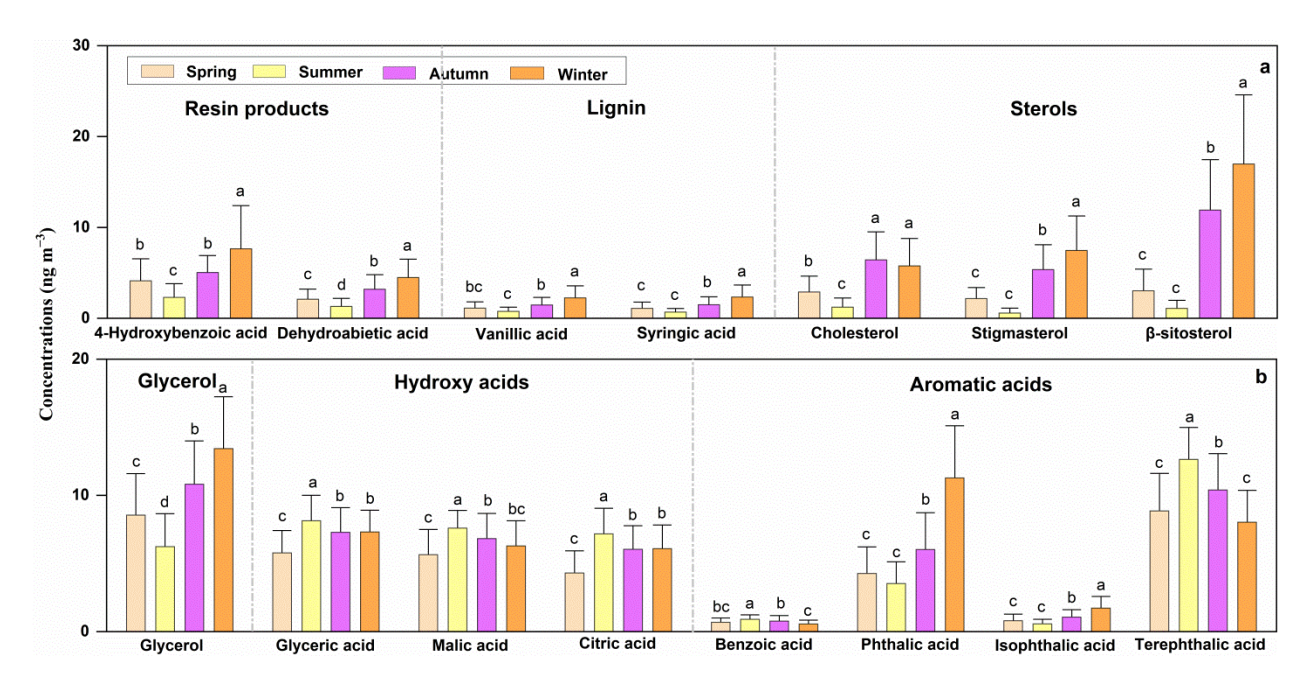


Figure 3. Molecular characteristics and seasonal variations of the minor polar compounds in $PM_{2.5}$. The explanations for the letters a, b, c, and d on the bars are provided in the caption of Figure 2.

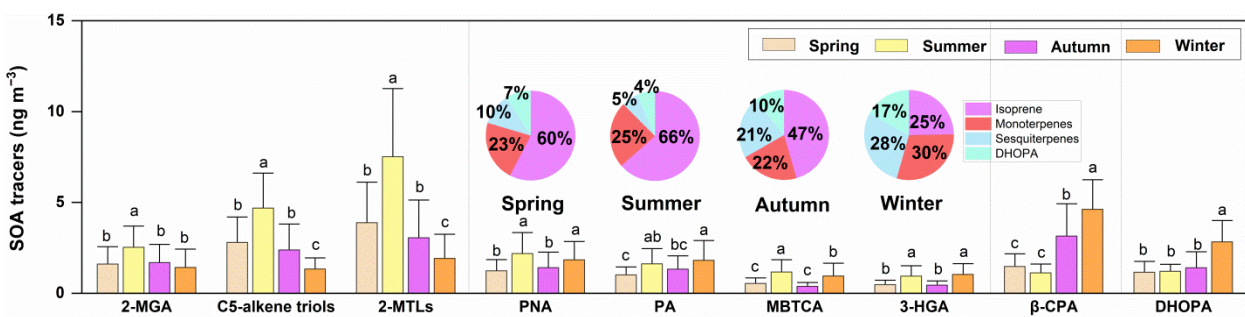


Figure 4. Molecular characteristics and seasonal variations of the SOA tracers in $PM_{2.5}$. The explanations for the letters a, b, c, and d on the bars are provided in the caption of Figure 2.

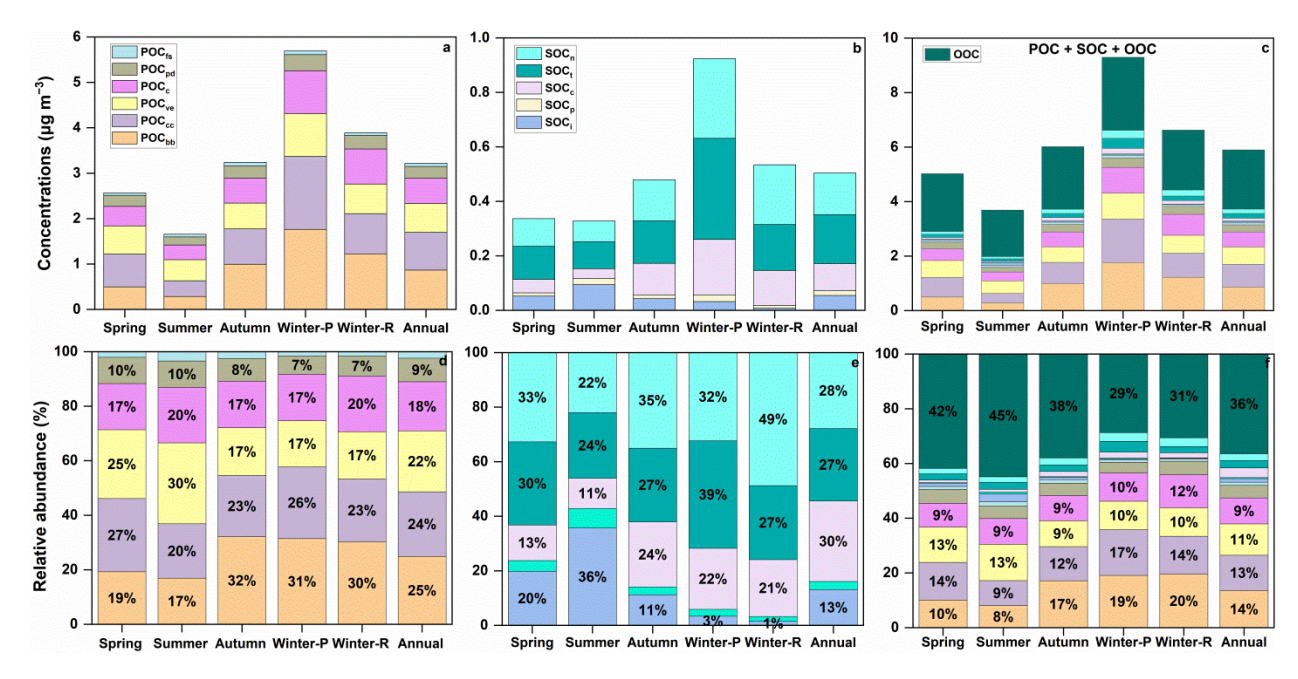


Figure 5. Concentrations and relative abundances of primary organic carbon (POC) from biomass burning (POC_{bb}), coal combustion (POC_{cc}), vehicle exhaust (POC_{ve}), cooking (POC_c), plant debris (POC_{pd}), and fungal spores (POC_{fs}), as well as secondary organic carbon (SOC) from isoprene (SOC_i), α/β -pinene (SOC_p), β -caryophyllene (SOC_c), toluene (SOC_t), and naphthalene (SOC_n). POC and SOC concentrations were estimated using a tracer-based method, while other organic carbon (OOC) was calculated by subtracting the estimated OC from the measured OC. Winter-P refers to winter pollution periods, and Winter-R denotes the winter remainder.

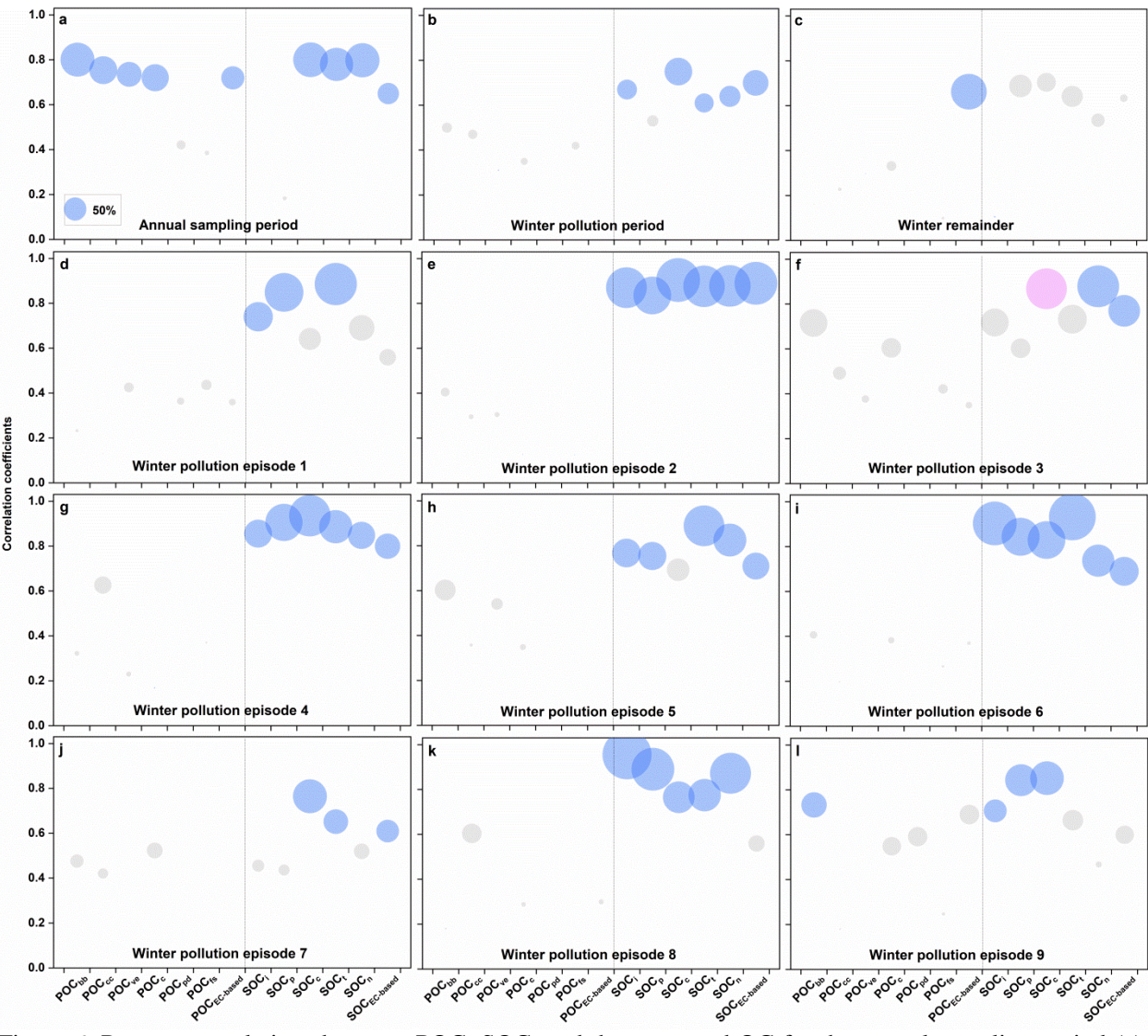


Figure 6. Pearson correlations between POC, SOC, and the measured OC for the annual sampling period (a), winter pollution periods (b), winter remainder (c), and individual pollution episodes in winter (d–l). The size of each circle represents the contribution (%) of POC and SOC to the variation in measured OC, as determined by redundancy analysis. Magenta circles indicate P-values from correlation and redundancy analyses less than 0.05, while gray circles denote P-values greater than 0.05. Definitions: POC_{bb} (biomass burning), POC_{cc} (coal combustion), POC_{ve} (vehicle exhaust), POC_c (cooking), POC_{pd} (plant debris), POC_{fs} (fungal spores), and POC_{EC-based} (based on the EC method). SOC_i, SOC_p, SOC_c, SOC_t, SOC_n, and SOC_{EC-based} correspond to SOC from isoprene, α/β-pinene, β-caryophyllene, toluene, naphthalene, and EC-based methods, respectively.

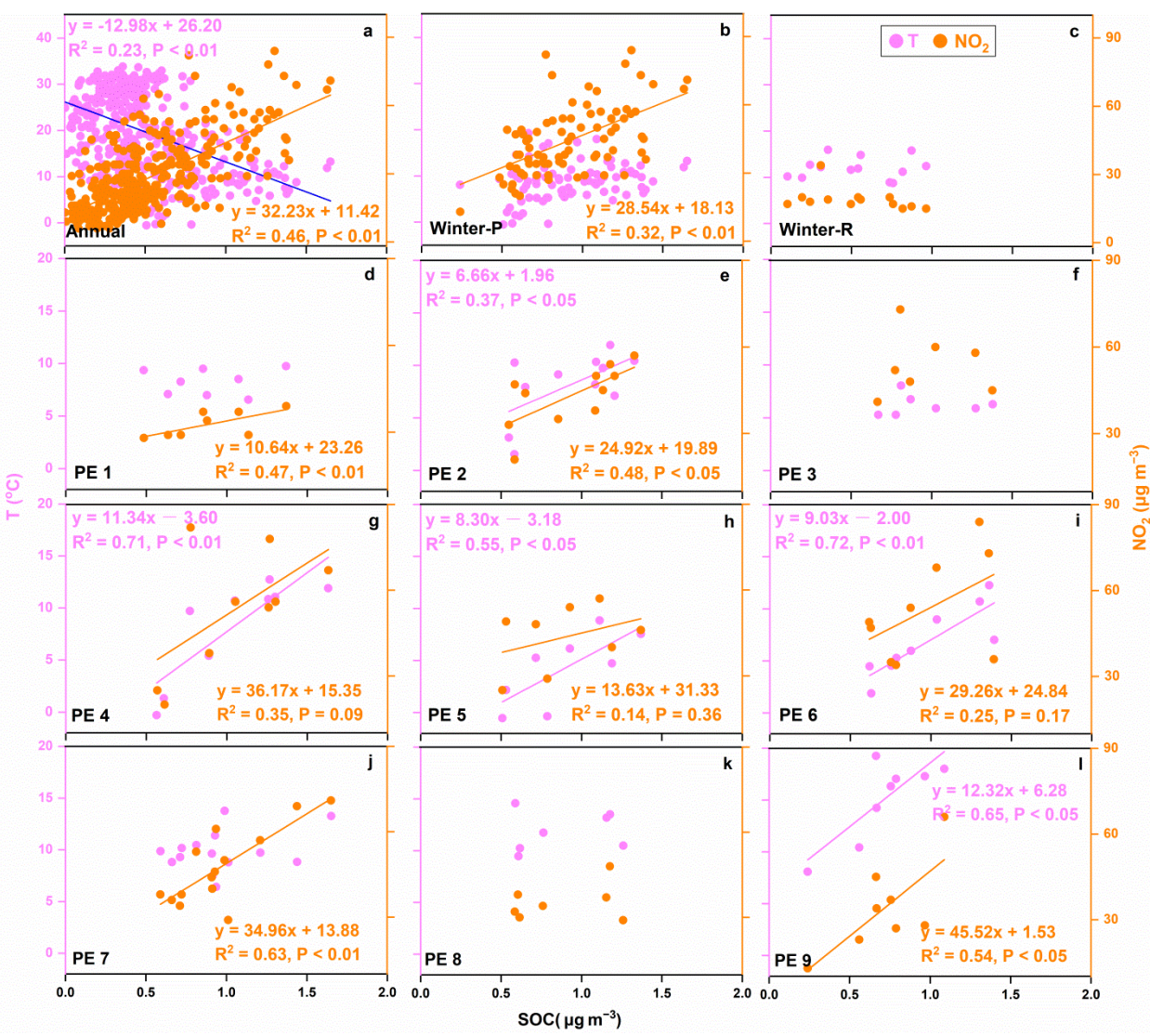


Figure 7. Linear correlations between temperature, NO₂, and SOC for the annual sampling periods (a), winter pollution periods (b), winter remainder (c), and individual winter pollution episodes (d–l). SOC concentrations were estimated using a tracer-based method. Winter-P refers to the winter pollution periods, while Winter-R denotes the winter remainder. PE1–PE9 correspond to winter pollution episodes 1–9.